

Selective Removal of Sodium Salt Taste Disrupts the Maintenance
of Dendritic Architecture of Second Order Taste Neurons in the Mouse
Nucleus of the Solitary Tract

Rolf Skyberg
Lakeville, MN

B.S. University of St. Thomas, 2013

A Dissertation Presented to the Graduate
Faculty of the University of Virginia in Candidacy for the Degree of
Doctor of Philosophy

Department of Psychology

University of Virginia
October 24th, 2018

Abstract

Neuronal activity plays critical roles in the development of sensory circuits in the mammalian brain. Recently, experimental manipulations have become available to alter gustatory activity from specific taste transduction pathways to investigate the roles taste experience play in the development of central gustatory circuits. Here we used a previously vetted mouse knockout model in which the transduction channel necessary for sodium taste is removed from taste bud cells throughout life. In these knockout mice, the terminal fields that carry taste information from the periphery into the nucleus of the solitary tract (NST) fail to develop, suggesting that neural sodium taste activity is important for the proper development of central gustatory circuits. Using this model, we tested the hypothesis that the development and maintenance of the dendritic architecture of NST relay cells, the primary postsynaptic partner of gustatory nerve terminal fields, are similarly dependent upon sodium taste activity from this single transduction pathway. The dendritic fields of NST relay cells, from adult male and female mice in which the α -subunit of the epithelial sodium channel was conditionally deleted in taste bud cells (α ENaC knockout mice) throughout life, were up to 2.4x larger and more complex than that of age-matched control mice. Interestingly, these differences in dendritic architecture were not present in postnatal day 20 (P20) mice of either sex. Overall, our results suggest that ENaC-mediated sodium taste activity is necessary for the maintenance of dendritic fields of relay cells in the gustatory NST.

Table of Contents

Chapter 1: Introduction.....	pg. 1
Neural Activity and Sensory System Development.....	pg. 2
Overview of Gustatory Circuitry.....	pg. 5
Development of Gustatory Circuitry.....	pg. 13
Citations.....	pg. 16
Figures.....	pg. 28
Chapter 2: Selective Removal of Sodium Salt Taste Disrupts the Maintenance of Dendritic Architecture of Second Order Taste Neurons in the Mouse Nucleus of the Solitary Tract.....	pg.34
Abstract.....	pg. 35
Significance Statement.....	pg. 36
Introduction.....	pg. 36
Materials and Methods.....	pg. 39
Results.....	pg. 50
Discussion.....	pg. 65
Citations.....	pg. 74
Figures.....	pg. 82
Chapter 3: Discussion and Comparison to Other Sensory Systems.....	pg. 92
Visual System.....	pg. 93
Auditory System.....	pg. 97
Concluding Remarks.....	pg. 98

Citations.....pg. 103

Chapter 1

One of the most astonishing features of the developing brain is its ability to structurally change in response to experience. While this anatomical plasticity underlies the development of many circuits in the brain, it is apparent in all sensory systems. In fact, the proper development of most sensory circuits is dependent upon appropriate levels of neural activity, without which circuits may develop abnormally or even fail to mature. For example, development of visual circuits that carry information from the retina to the first central synapse, in the dorsal lateral geniculate nucleus (dLGN), are dependent upon neural activity generated in retinal ganglion cells (Grubb et al., 2003; Pfeiffenberger et al., 2005; Huberman et al., 2008). Without this normal retinal activity these retinogeniculate circuits exhibit abnormal terminal fields, synaptic connectivity, and physiology (Katz and Shatz, 1996; Grubb et al., 2003; McLaughlin et al., 2003; Chandrasekaran et al., 2005; Hooks and Chen, 2006; Guido, 2008). Neural activity also plays a similar role in the development of gustatory afferent nerves that carry taste information from taste buds to the first central synapse, in the nucleus of the solitary tract (NST)(Hill and Bour, 1985; Vogt and Hill, 1993; Mangold and Hill, 2008; Corson and Hill, 2011; Sun et al., 2017). However, the structural and functional details of the development of this circuit are not well understood.

The overall aim of this project was to identify how neural activity impacts the anatomical development of gustatory circuits in the brainstem throughout life. The following studies will accomplish this in three ways. First, I will test the hypothesis that deletion of sodium-taste activity throughout development, which

results in abnormally large terminal field volumes of gustatory nerves, will be reflected in changes in the dendritic organization of NST relay neurons in adult mice. Second, I will begin to establish when structural changes occur during development by investigating both the presynaptic terminal field size as well as the dendritic organization of the postsynaptic NST relay neurons in immature mice before a time in which normal peripheral taste activity has matured. And finally, by recording whole nerve activity, I will characterize the development of peripheral sodium taste elicited activity in control animals as well as confirm the effectiveness of our genetic knockout model. These studies will not only further our understanding of how taste circuits within the brainstem develop but will also provide the foundation for future experiments investigating the role of neural activity in the development, maintenance, and plasticity of neural circuits throughout the brain both during development and at adulthood.

In this introductory chapter, an overview of the roles neural activity plays in the development of sensory systems, particularly the visual system, will be presented. Following this, an introduction to the gustatory system circuitry and development will be provided, with a primary focus on circuits that carry taste information from taste buds to the brain. Collectively, these sections will provide the background and rationale for the experiments proposed in Chapter 2.

Neural Activity and Sensory System Development

Neural activity plays an integral role in the proper development of sensory circuits in the central nervous system (Brunjes, 1994; Lee et al., 2005; Leake et al.,

2006; Sun et al., 2017). While this activity-dependent development can be seen at some level in every sensory system, it has been the most thoroughly researched in the visual system. Both cortical and subcortical nuclei involved in visual processing demonstrate a dependence upon visually-evoked neural activity for proper circuit organization to occur (Wiesel and Hubel, 1963; Katz and Shatz, 1996; Guido, 2008; Wang et al., 2015). This dependence is exemplified by the circuitry of the dLGN, a thalamic relay and one of the first central synaptic nuclei of the visual system. Retinal ganglion cells project from the eyes to both the ipsilateral and contralateral dLGN, where they initially create diffuse terminal fields (Hooks and Chen, 2007; Guido, 2008). Through a refinement period, driven by both spontaneous and visually-evoked retinal activity, these terminal fields segregate into eye-specific layers (Katz and Shatz, 1996; Hooks and Chen, 2006; Guido, 2008). Pharmacological, surgical, or genetic removal of spontaneous retinal activity, visually-evoked neural activity, or both can prevent the segregation of inputs into eye-specific layers (Grubb et al., 2003; Pfeiffenberger et al., 2005; Hooks and Chen, 2006, 2008; Guido, 2008; Huberman et al., 2008). Therefore, proper refinement of these afferent inputs is dependent upon both spontaneous and visually-evoked retinal activity. As one might expect, retinal ganglion cell (RGC) axons are not the only part of dLGN circuitry that exhibit this dependence on neural activity. The primary recipient of RGC input, thalamocortical relay cells, may also develop in an activity-dependent fashion. Removing visually-evoked activity during critical developmental periods in kittens via monocular deprivation has been reported to alter thalamocortical dendritic morphology in monkeys (Matthews et al., 1960) and kittens (Wiesel and

Hubel, 1963). This suggests that the development of proper dendritic morphology in thalamocortical relay cells is somewhat dependent upon retinal activity. Finally, retinal activity also drives the development of synaptic connections between RGC axons and thalamocortical relay cells in the dLGN (Stellwagen and Shatz, 2002; Butts et al., 2007; Guido, 2008; Thompson et al., 2017). In developing mice, with normal retinal inputs, a single thalamocortical relay cell initially forms functional synapses with up to two dozen RGCs from both eyes (Chen and Regehr, 2000; Jaubert-Miazza et al., 2005; Ziburkus and Guido, 2006). Throughout the following weeks this connectivity is reduced to receiving input from one to three RGCs (Jaubert-Miazza et al., 2005; Guido, 2008), and almost none of these cells receive binocular inputs (Ziburkus and Guido, 2006). This sculpting of dLGN synapses is driven by retinal activity, both spontaneous and visually-evoked (Stellwagen and Shatz, 2002; Jaubert-Miazza et al., 2005; Butts et al., 2007; Hooks and Chen, 2008; Dilger et al., 2015; Thompson et al., 2017).

Interestingly, circuitry in the superior colliculus (SC), the other primary synaptic nucleus within the visual system, exhibits a similar dependence upon neural activity to develop properly. RGC terminal fields in the SC develop ectopically when spontaneous retinal activity is disrupted throughout life, resulting in large diffusely organized terminal fields in adulthood (McLaughlin et al., 2003; Chandrasekaran et al., 2005). Furthermore, removal of spontaneous retinal activity also disrupts the development of receptive field properties of neurons in the SC that respond to visual stimuli (Cang et al., 2005; Chandrasekaran et al., 2005; Mrsic-Flogel, 2005; Wang et al., 2009). These alterations in the receptive field properties of

SC neurons imply that disrupting retinal activity alters more than just the developing RGC terminal fields (i.e. dendritic architecture of cells within the SC and/or alterations in the organization of synapses within the circuit).

In summary, neural activity generated in the retina has multiple effects on the development of dLGN and SC circuitry. Without which, RGC axons in the dLGN and SC do not organize into eye-specific layers (Grubb et al., 2003; McLaughlin et al., 2003; Chandrasekaran et al., 2005; Pfeiffenberger et al., 2005; Hooks and Chen, 2007, 2008; Guido, 2008; Huberman et al., 2008), thalamocortical relay cell dendrites develop ectopically (Matthews et al., 1960; Wiesel and Hubel, 1963), synaptic input onto thalamocortical relay cells remains broad and binocularly driven (Stellwagen and Shatz, 2002; Jaubert-Miazza et al., 2005; Butts et al., 2007; Guido, 2008; Hooks and Chen, 2008; Dilger et al., 2015; Thompson et al., 2017), and receptive fields of SC relay neurons exhibit abnormal patterns of connectivity (Chandrasekaran et al., 2005; Mrsic-Flogel, 2005; Wang et al., 2009, 2015). Gustatory circuitry, while not identical, shares many of the same organizational and developmental patterns that have been discovered in the visual circuit.

Overview of Gustatory Circuitry

The mammalian gustatory system is responsible for the evaluation of the nutrient content of food as well as preventing the ingestion of potentially toxic chemicals. Transduction of taste stimuli occurs through multiple molecular pathways in taste bud cells, which are anatomically organized in a garlic bulb-like structure to create taste buds on the surface of the tongue and throughout the oral cavity. Though there are subtle regional differences in the sensitivity to differing

tastants, most taste buds are broadly tuned to many taste stimuli and therefore serve similar functions (Lindemann, 1999; Spector and Travers, 2005; Chaudhari and Roper, 2010). The chorda tympani (CT), greater superficial petrosal (GSP), and glossopharyngeal (IX) nerves innervate these taste buds and carry taste-related neural activity from the periphery to the NST in the brainstem. Within the rodent NST, these three gustatory afferents create overlapping terminal fields, which synapse onto NST relay cells that process this neural information before projecting to the parabrachial nucleus (PBN). From the PBN, a majority of the gustatory pathway continues to the ventral posteromedial thalamus (VPMpc) and then to the gustatory cortex (GC) in the insula (Fig. 1)(Wolf, 1968; Fulwiler and Saper, 1984). However, there are PBN projections leading directly to the insula, lateral hypothalamus, bed nucleus of the stria terminalis, and central nucleus of the amygdala (Norgren, 1974, 1976; Bernard et al., 1993). The latter pathway likely carries hedonic information, while the former pathway is more devoted to feature extraction of the stimulus concentration and identity (Grill and Norgren, 1978; Spector and Travers, 2005)

Gustatory Nerves

While the CT, GSP, and IX nerves all transmit taste related information, they are by no means a functionally homogenous assemblage of fibers. Each nerve receives input from distinct topographic regions of the oral cavity, exhibits differing physiological sensitivities for gustatory and non-gustatory stimuli, and innervates distinct, albeit overlapping, regions within the NST (Spector and Travers, 2005;

Chandrashekar et al., 2010; Chaudhari and Roper, 2010; Sun et al., 2015, 2017; Skyberg et al., 2017).

The CT innervates taste buds in fungiform papillae on the anterior tongue as well as antero-most foliate papillae on the posterior tongue (Whiteside, 1927; Yamamoto and Kawamura, 1975). It is a branch of the VII cranial nerve and houses its cell somas in the geniculate ganglia (Fig. 1). CT fibers respond to gustatory, thermal, and mechanical stimuli, although the majority of fibers are maximally responsive to taste stimuli (Pfaffmann, 1941; Biedenbach and Chan, 1971; Shingai and Beidler, 1985; Matsuo et al., 1995). The rodent CT responds well to many concentrations of the prototypical stimuli that represent salty, sour, sweet, and umami (Shingai and Beidler, 1985; Finger et al., 2005; Chandrashekar et al., 2010; Sun et al., 2015, 2017; Skyberg et al., 2017), but does not respond well to bitter stimuli (Shingai and Beidler, 1985). Importantly, CT responses to varying concentrations of salty solutions are significantly attenuated by lingual application of the epithelial sodium channel (ENaC) blocker, amiloride (Hill and Bour, 1985; Sollars and Hill, 1998; Skyberg et al., 2017; Sun et al., 2017). This demonstrates that the high sensitivity of the CT to sodium stimuli is due to an ENaC-gated transduction pathway. The CT enters the rostral NST and sends terminal processes medially. When the brainstem is sectioned horizontally, CT axons are found throughout the dorsal-ventral axis, but they have a strong spatial preference for intermediate and ventral aspects of this axis (Fig. 2)(Sun et al., 2015, 2017; Skyberg et al., 2017).

The GSP nerve innervates taste buds located in the nasoincisor duct, the geschmacksstreifen (GS) and the soft palate, all located along the roof of the oral

cavity. Like the CT, the GSP is a branch of the VII cranial nerve and houses its cell soma in the geniculate ganglia (Fig. 1). The GSP demonstrates similar response properties to what has been observed in the CT. Oral application of sucrose, acids, salts and, to a lesser extent, quinine are all capable of producing neural responses in the GSP (Hill and Bour, 1985; Shingai and Beidler, 1985; Nejad, 1986; Harada et al., 1997; Sollars and Hill, 1998; Finger et al., 2005; Skyberg et al., 2017; Sun et al., 2017). Sodium taste responses in the GSP are also susceptible to attenuation by amiloride, again showing the important role that ENaCs play in the transduction of sodium taste stimuli in this nerve (Skyberg et al., 2017; Sun et al., 2017). Less is known about the extent to which mechanical or thermal stimuli are able to drive GSP activity. Like the CT, the GSP innervates the entirety of the dorsal-ventral axis of the rostral NST in horizontal sections. However, GSP innervations are found further dorsal than CT axons and are less prevalent in the ventral portion of the NST than CT axons (Fig. 2)(Sun et al., 2015, 2017; Skyberg et al., 2017).

The IX nerve innervates taste buds in posterior foliate and circumvallate papillae on the posterior tongue and has its cell bodies in the petrosal ganglia (Fig. 1). Nerve IX responds best to bitter stimuli and to a lesser extent acids, sugars and salts (Shingai and Beidler, 1985; Ninomiya et al., 1993; Ninomiya, 1998; Danilova, 2003; Skyberg et al., 2017). Importantly, relative to the salt responses generated in the CT and GSP, IX responses are very small, requiring significantly higher stimulus concentrations to produce responses, and are not amiloride sensitive (Formaker and Hill, 1991; Doolin and Gilbertson, 1996; Ninomiya, 1998; Skyberg et al., 2017). IX axons preferentially innervate the dorsal-most aspects of the NST in horizontal

sections and tend to avoid the ventral portion of the nucleus (Fig. 2)(Sun et al., 2015, 2017; Skyberg et al., 2017). This trend is especially true when comparing these innervation patterns to those of the CT and GSP.

Nucleus of the Solitary Tract

The NST is the first central synaptic relay within the taste system, and, thus, plays an important role in the sensory coding of taste as well as driving feeding and motivated behaviors associated with taste (Spector and Travers, 2005; Spector and Glendinning, 2009). In the horizontal plane, the NST envelops the caudal portion of the fourth ventricle, giving it a V shape (Fig. 3A). The solitary tract is located along the lateral edge of the nucleus, and terminal fields from gustatory afferent fibers project medially from the rostral edge of the solitary tract into the rostral NST (Fig. 3A)(Sun et al., 2015, 2017; Skyberg et al., 2017). It is within this rostral portion of NST that CT, GSP, and IX all synapse onto postsynaptic targets.

In the coronal plane, the NST has been divided into four major subdivisions: the rostrocentral, rostrolateral, medial, and the ventral subdivisions (Fig. 3B and C). These four subdivisions have been defined by their cellular characteristics (Whitehead, 1988, 1990), patterns of afferent and efferent connectivity (King and Hill, 1993; Halsell and Travers, 1997; Whitehead et al., 2000; King, 2007; Corson et al., 2012), and function (Harrer and Travers, 1996; DiNardo and Travers, 1997; King et al., 1999; Travers, 2002; King, 2007). Briefly, the rostrocentral, and somewhat less, rostrolateral subdivision receive the majority of gustatory related information from the periphery and have been the target of much interest in regards to the

gustatory circuitry (Norgren and Leonard, 1973; Hamilton and Norgren, 1984; King, 2007; Corson et al., 2012; Corson and Erisir, 2013). The medial subdivision is also innervated by gustatory afferent fibers and plays a role in combining viscerosensory and gustatory information (Beckman and Whitehead, 1991; King, 2007). The ventral subdivision regulates the oromotor reflex associated with aversive gustatory stimuli (Travers, 1988; Halsell and Travers, 1997; King, 2007). Given that this thesis is focused on how changes in taste elicited neural activity alter NST circuitry, I will focus on the rostrocentral and rostrolateral subdivisions, which receive the majority of monosynaptic input from the gustatory afferents.

Cells in the Nucleus of the Solitary Tract

Cells within the rostrocentral and rostrolateral subdivisions that receive ascending gustatory input are a heterogeneous population. These cells have classically been divided into three basic morphological classes: ovoid, elongate (bipolar), and stellate (multipolar) (Fig. 4)(Davis and Jang, 1988; Whitehead, 1988; Whitehead et al., 1993; King and Bradley, 1994; King, 2007). All three classes of cells receive glutamatergic synaptic contacts from gustatory afferents (Whitehead, 1993) though only elongate and stellate cells project out of the NST, while ovoid cells are local GABAergic interneurons (Lasiter and Kachele, 1988; Wang and Bradley, 1993, 1995; Bradley et al., 1996; Grabauskas and Bradley, 1996; Renehan et al., 1996; Li and Smith, 1997; Bradley and Grabauskas, 1998; Smith et al., 1998). While stellate and elongate cells both receive and transmit gustatory information out of the NST, they exhibit a few key differences. First, elongate (bipolar) cells only have two long,

simple, primary dendrites projecting from either side of the cell soma, typically along the medial-lateral axis (Fig. 4C)(Whitehead, 1988; King and Bradley, 1994). Stellate (multipolar) cells, on the other hand, average between three to five primary dendrites that exhibit a greater complexity than elongate cells (Fig. 4B)(Davis and Jang, 1988; Whitehead, 1988; King and Bradley, 1994). These dendrites project from the cell soma in all directions but tend to orient themselves in the horizontal plane, primarily extending in the rostral-caudal direction (Whitehead, 1988; King and Bradley, 1994; Corson and Erisir, 2013). This dendritic orientation aligns these cells parallel to the solitary tract, placing them directly in the path of ascending gustatory afferents, suggesting that these cells are the recipients of afferent gustatory information. In fact, electrophysiological studies of stellate cells show that these cells are broadly tuned and receive convergent information from more than one of the gustatory nerves (Travers et al., 1986; Sweazey and Bradley, 1989; Mistretta and Labyak, 1994; Bradley et al., 1996; Rosen and Di Lorenzo, 2012). A second key difference between these two cellular populations is their location within the subdivisions of the NST. Elongate cells are present in both the rostrocentral and rostrolateral NST subdivisions; however, they show a spatial tendency towards being in the latter subdivision (Whitehead, 1988; King and Bradley, 1994; Halsell and Travers, 1997; King, 2007). Stellate cells show a slight spatial preference for the rostrocentral subdivision, though their dendrites often extend outside of region (Whitehead, 1988; King, 2007). Interestingly, non-gustatory orosensory information tends to excite cells in the rostrolateral NST subdivision, alluding to a role for elongate cells as processors of this particular type of information (Whitehead, 1988;

Corson et al., 2012; Breza and Travers, 2016). A final difference between these two cellular populations, or more accurately these two NST subdivisions, is their projection patterns to the PBN (Norgren and Leonard, 1973; Van Buskirk and Smith, 1981; Whitehead, 1990; Halsell and Travers, 1997; Tokita et al., 2009).

Parabrachial Nucleus

The PBN is the second central synaptic relay within the rodent central taste circuit and receives ascending taste-related neural activity from the NST as well as descending taste-related neural activity from cortical structures involved in taste processing (Fig. 1)(Whitehead, 1990; Halsell and Travers, 1997; Tokita et al., 2009; Tokita and Boughter, 2016). Ascending fibers originating in the rostrocentral NST innervate the “waist” region of the PBN, making it the primary taste-responsive portion of the PBN (Fig. 5)(Norgren and Leonard, 1973; Halsell and Travers, 1997; Tokita et al., 2009). Electrophysiological studies support the idea that the “waist” region of the PBN receives a majority of the ascending taste-elicited neural activity (Norgren and Leonard, 1973; Halsell and Travers, 1997; Tokita and Boughter, 2016). However, ascending fibers from the rostralateral NST also innervate the external subregions of the PBN. As was noted previously, this circuit seems to be involved in nongustatory, orosensory processing (Halsell and Travers, 1997). The PBN sends ascending projections primarily to the gustatory thalamic relay (VPMpc), but also sends smaller projections to the insula, lateral hypothalamus, bed nucleus of the stria terminalis, and central nucleus of the amygdala (Fig. 1)(Norgren, 1974; Bernard et al., 1993). Along with these ascending projections, the PBN also sends

descending projections to the NST, making the a reciprocal NST-PBN connection (Karimnamazi and Travers, 1998; Kang and Lundy, 2009; Tokita et al., 2009).

Development of Gustatory Circuitry

During normal development, gustatory circuits in the rodent NST undergoes significant changes both anatomically and physiologically. Initially, the terminal fields of the CT, GSP, and IX in the NST are large and overlap extensively with each other. However, from postnatal day 15 (P15) to P35, the CT and GSP terminal fields are “pruned” into a smaller, more segregated, mature organization (Fig. 6A)(Sollars et al., 2006; Mangold and Hill, 2008; Zheng et al., 2014). After P35, these terminal fields do not change significantly. Interestingly this period of terminal field reorganization closely follows the period when ENaC-mediated sodium taste stimuli become progressively more effective in driving neural responses in the CT (Fig. 6B) (Hill and Bour, 1985; Zheng et al., 2014), and probably in driving neural responses in the GSP. Nerve IX, which is not highly sodium sensitive, and does not innervate taste buds with functional ENaCs (Doolin and Gilbertson, 1996; Ninomiya, 1998; Skyberg et al., 2017), and has a terminal field that is mature by P15 (Fig. 6A)(Zheng et al., 2014). Thus, ENaC-mediated neural activity likely plays an important role in driving the development of CT and GSP terminal fields in the NST, and the absence of this channel leads to a lack of “pruning” with age. Recently Sun et al., (2017) demonstrated that the development of terminal fields was, in fact, dependent on normal levels of sodium taste activity. By selectively eliminating functional ENaCs in taste buds throughout pre- and postnatal development, the CT, GSP, and IX terminal

fields in these ENaC KO mice were up to 2x larger than age-matched controls at adulthood. Moreover, the maintenance of CT and GSP terminal fields at adulthood are dependent upon normal levels of ENaC-mediated sodium taste activity (Skyberg et al., 2017). When taken together, the above findings reveal a developmental and organizational role for a single transduction pathway in the rodent gustatory system. Without sodium taste activity throughout life, CT and GSP terminal fields do not “prune” into a mature state (Sun et al., 2017). Also, deletion of ENaC-mediated neural activity at adulthood, leads to an expansion of CT and GSP terminal fields that is similar to that found in immature mice (Skyberg et al., 2017). Therefore, gustatory afferents exhibit high levels of plasticity throughout an animal’s life (May and Hill, 2006; Corson and Hill, 2011; Sun et al., 2015, 2017; Skyberg et al., 2017).

Less is known about the extent to which this plasticity exists in other parts of the NST gustatory circuit. Given the large effects that removing a single taste modality has on gustatory terminal fields and the roles neural activity have on other sensory systems, one might expect further effects of removal of ENaC-mediated neural activity on gustatory circuitry in the NST. In fact, there are studies suggesting that taste-elicited neural activity plays a role in the development of the dendritic architecture of NST cells that receive inputs from gustatory nerves (i.e., postsynaptic to the terminal fields described above)(Lasiter and Kachele, 1990; Lasiter, 1991). However, these studies fall short of conclusively proving so for a few reasons. First, these studies attempt to alter taste-elicited activity by damaging (i.e., burning) peripheral receptors throughout the anterior tongue. While this damage destroys gustatory receptors throughout the lingual surface of the tongue, it more than likely

also damages progenitor cells for taste buds and the gustatory fibers carrying taste related information to the NST. Therefore, the effects of this manipulation cannot be directly attributed to a specific reduction in taste-elicited neural activity. Second, evidence for global effects are supported because the effects of this damage persist even after the taste buds at least partially regenerate. Finally, the normal developmental pattern shown for CT terminal fields in these studies are opposite to what have been reported from our lab. That is, they show an age-dependent increase in terminal field size rather than “pruning” of the fields with age. Thus, it is not clear how applicable these data are to our knowledge of the development and plasticity of gustatory circuits in the NST. The research presented in Chapter 2 is designed to address the hypothesis that taste elicited neural activity plays a role in the overall development and organization of gustatory circuitry within the NST.

Citations

- Beckman ME, Whitehead MC (1991) Intramedullary connections of the rostral nucleus of the solitary tract in the hamster. *Brain Res* 557:265–279.
- Bernard J -F, Alden M, Besson J -M (1993) The organization of the efferent projections from the pontine parabrachial area to the amygdaloid complex: A phaseolus vulgaris leucoagglutinin (PHA-L) study in the rat. *J Comp Neurol* 329:201–229.
- Biedenbach MA, Chan KY (1971) Tongue mechanoreceptors: comparison of afferent fibers in the lingual nerve and chorda tympani. *Brain Res* 35:584–588.
- Bradley RM, Grabauskas G (1998) Neural circuits for taste. Excitation, inhibition, and synaptic plasticity in the rostral gustatory zone of the nucleus of the solitary tract. *Ann N Y Acad Sci* 855:467–474.
- Bradley RM, King MS, Wang L, Shu X (1996) Neurotransmitter and neuromodulator activity in the gustatory zone of the nucleus tractus solitarius. *Chem Senses* 21:377–385.
- Breza JM, Travers SP (2016) P2X2 receptor terminal field demarcates a “transition zone” for gustatory and mechanosensory processing in the mouse nucleus tractus solitarius. *Chem Senses* 41:515–524.
- Butts DA, Kanold PO, Shatz CJ (2007) A burst-based “Hebbian” learning rule at retinogeniculate synapses links retinal waves to activity-dependent refinement. *PLoS Biol* 5:0651–0661.
- Brunjes P (1994) Unilateral naris closure and olfactory system development. *Brain Res Rev* 19:146–160.

- Cang J, Rentería RC, Kaneko M, Liu X, Copenhagen DR, Stryker MP (2005) Development of precise maps in visual cortex requires patterned spontaneous activity in the retina. *Neuron* 48:797–809.
- Chandrasekaran AR, Plas D, Gonzalez E, Crair MC (2005) Evidence for an Instructive Role of Retinal Activity in Retinotopic Map Refinement in the Superior Colliculus of the Mouse. *J Neurosci* 25:6929–6938.
- Chandrashekar J, Kuhn C, Oka Y, Yarmolinsky D a, Hummler E, Ryba NJP, Zuker CS (2010) The cells and peripheral representation of sodium taste in mice. *Nature* 464:297–301.
- Chaudhari N, Roper SD (2010) The cell biology of taste. *J Cell Biol* 190:285–296.
- Chen C, Regehr WG (2000) Developmental Remodeling of the Retinogeniculate Synapse. *J Neurosci* 20:955–966.
- Corson JA, Erisir A (2013) Monosynaptic convergence of chorda tympani and glossopharyngeal afferents onto ascending relay neurons in the nucleus of the solitary tract: A high-resolution confocal and correlative electron microscopy approach. *J Comp Neurol* 521:2907–2926.
- Corson J, Aldridge A, Wilmoth K, Erisir A (2012) A survey of oral cavity afferents to the rat nucleus tractus solitarii. *J Comp Neurol* 520:495–527.
- Corson SL, Hill DL (2011) Chorda Tympani Nerve Terminal Field Maturation and Maintenance Is Severely Altered Following Changes to Gustatory Nerve Input to the Nucleus of the Solitary Tract. *J Neurosci* 31:7591–7603.
- Danilova V (2003) Comparison of the responses of the chorda tympani and glossopharyngeal nerves to taste stimuli in C57BL/6J mice. *J Neurosci* 23:1–15.

- Davis BJ, Jang T (1988) A Golgi analysis of the gustatory zone of the nucleus of the solitary tract in the adult hamster. *J Comp Neurol* 278:388–396.
- Dilger EK, Krahe TE, Morhardt DR, Seabrook T a., Shin H-S, Guido W (2015) Absence of Plateau Potentials in dLGN Cells Leads to a Breakdown in Retinogeniculate Refinement. *J Neurosci* 35:3652–3662.
- DiNardo LA, Travers JB (1997) Distribution of Fos-Like Immunoreactivity in the Medullary Reticular Formation of the Rat after Gustatory Elicited Ingestion and Rejection Behaviors. *J Neurosci* 17:3826 LP-3839.
- Doolin RE, Gilbertson T a (1996) Distribution and characterization of functional amiloride-sensitive sodium channels in rat tongue. *J Gen Physiol* 107:545–554.
- El-Danaf RN, Krahe TE, Dilger EK, Bickford ME, Fox MA, Guido W (2015) Developmental remodeling of relay cells in the dorsal lateral geniculate nucleus in the absence of retinal input. *Neural Dev* 10:1–17.
- Finger TE, Danilova V, Barrows J, Bartel DL, Vigers AJ, Stone L, Hellekant G, Kinnamon SC (2005) ATP signaling is crucial for communication from taste buds to gustatory nerves. *Science* 310:1495–1499.
- Formaker BK, Hill DL (1991) Lack of amiloride sensitivity in SHR and WKY glossopharyngeal taste responses to NaCl. *Physiol Behav* 50:765–769.
- Fulwiler CE, Saper CB (1984) Subnuclear organization of the efferent connections of the parabrachial nucleus in the rat. *Brain Res Rev* 7:229–259.
- Grabauskas G, Bradley RM (1996) Synaptic interactions due to convergent input from gustatory afferent fibers in the rostral nucleus of the solitary tract. *J Neurophysiol* 76:2919–2927.

- Grill HJ, Norgren R (1978) The Taste reactivity test. II. Mimetic responses to gustatory stimuli in chronic thalamic and chronic decerebrate rats. *J Neurosci* 143:281–297.
- Grubb MS, Rossi FM, Changeux JP, Thompson ID (2003) Abnormal functional organization in the dorsal lateral geniculate nucleus of mice lacking the beta 2 subunit of the nicotinic acetylcholine receptor. *Neuron* 40:1161–1172.
- Guido W (2008) Refinement of the retinogeniculate pathway. *J Physiol* 586:4357–4362.
- Halsell CB, Travers SP (1997) Anterior and posterior oral cavity responsive neurons are differentially distributed among parabrachial subnuclei in rat. *J Neurophysiol* 78:920–938.
- Hamilton RB, Norgren R (1984) Central projections of gustatory nerves in the rat. *J Comp Neurol* 222:560–577.
- Harada S, Yamamoto T, Yamaguchi K, Kasahara Y (1997) Different Characteristics of Gustatory Responses Between the Greater Superficial Petrosal and Chorda Tympani Nerves in the Rat. *Chem Senses* 22:133–140.
- Harrer MI, Travers SP (1996) Topographic organization of Fos-like immunoreactivity in the rostral nucleus of the solitary tract evoked by gustatory stimulation with sucrose and quinine. *Brain Res* 711:125–137.
- Hill DL, Bour TC (1985) Addition of functional amiloride-sensitive components to the receptor membrane: A possible mechanism for altered taste responses during development. *Dev Brain Res* 20:310–313.
- Hooks BM, Chen C (2006) Distinct Roles for Spontaneous and Visual Activity in

- Remodeling of the Retinogeniculate Synapse. *Neuron* 52:281–291.
- Hooks BM, Chen C (2007) Critical periods in the visual system: changing views for a model of experience-dependent plasticity. *Neuron* 56:312–326.
- Hooks BM, Chen C (2008) Vision Triggers an Experience-Dependent Sensitive Period at the Retinogeniculate Synapse. *J Neurosci* 28:4807–4817.
- Huberman AD, Feller MB, Chapman B, Manuscript A, Microbiología D, Rica UDC, José S, Rica C, Manuscript A, Huberman AD, Feller MB, Chapman B (2008) Mechanisms Underlying Development of Visual Maps and Receptive Fields. *Annu Rev Neurosci* 31:479–509.
- Jaubert-Miazza L, Green E, Lo FS, Bui K, Mills J, Guido W (2005) Structural and functional composition of the developing retinogeniculate pathway in the mouse. *Vis Neurosci* 22:661–676.
- Kang Y, Lundy RF (2009) Terminal field specificity of forebrain efferent axons to brainstem gustatory nuclei. *Brain Res* 1248:76–85.
- Karimnamazi H, Travers JB (1998) Differential projections from gustatory responsive regions of the parabrachial nucleus to the medulla and forebrain. *Brain Res* 813:283–302.
- Katz L., Shatz CJ (1996) Synaptic Activity and the Construction of Cortical Circuits. *Science* 274:1133–1138.
- King CT, Hill DL (1993) Neuroanatomical alterations in the rat nucleus of the solitary tract following early maternal NaCl deprivation and subsequent NaCl repletion. *J Comp Neurol* 333:531–542.
- King CT, Travers SP, Rowland NE, Garcea M, Spector AC (1999) Glossopharyngeal

- Nerve Transection Eliminates Quinine-Stimulated Fos-Like Immunoreactivity in the Nucleus of the Solitary Tract: Implications for a Functional Topography of Gustatory Nerve Input in Rats. *J Neurosci* 19:3107 LP-3121.
- King MS (2007) Anatomy of the Rostral Nucleus of the Solitary Tract. :1–16.
- King MS, Bradley RM (1994) Relationship between structure and function of neurons in the rat rostral nucleus tractus solitarii. *J Comp Neurol* 344:50–64.
- Lasiter PS (1991) Effects of early postnatal receptor damage on dendritic development in gustatory recipient zones of the rostral nucleus of the solitary tract. *Dev Brain Res* 61:197–206.
- Lasiter PS, Kachele DL (1988) Organization of GABA and GABA-transaminase containing neurons in the gustatory zone of the nucleus of the solitary tract. *Brain Res Bull* 21:623–636.
- Lasiter PS, Kachele DL (1990) Effects of early postnatal receptor damage on development of gustatory recipient zones within the nucleus of the solitary tract. *Dev Brain Res*:57–71.
- Leake P, Hradek G, Chair L, Snyder R (2006) Neonatal deafness results in degraded topographic specificity of auditory nerve projections to the cochlear nucleus in cats. *J Comp Neurol* 497:13–31.
- Lee L-J, Lo F-S, Erzurumlu R (2005) NMDA Receptor-Dependent Regulation of Axonal and Dendritic Branching. *J Neurosci* 25:2304–2311.
- Li CS, Smith D V (1997) Glutamate receptor antagonists block gustatory afferent input to the nucleus of the solitary tract. *J Neurophysiol* 77:1514–25.
- Lindemann B (1999) Receptor seeks ligand: On the way to cloning the molecular

receptors for sweet and bitter taste. *Nat Med* 5:381–382.

Mangold JE, Hill DL (2008) Postnatal reorganization of primary afferent terminal fields in the rat gustatory brainstem is determined by prenatal dietary history. *J Comp Neurol* 509:594–607.

Matsuo R, Inoue T, Masuda Y, Nakamura O, Yamauchi Y, Morimoto T (1995) Neural activity of chorda tympani mechanosensitive fibers during licking behavior in rats. *Brain Res* 689:289–298.

Matthews MR, Cowan WM, Powell TPS (1960) Transneuronal cell degeneration in the lateral geniculate nucleus of the macaque monkey. *J Anat* 94:145–169.

May O, Hill DL (2006) Gustatory terminal field organization and developmental plasticity in the nucleus of the solitary tract revealed through triple fluorescence labeling. *J Comp Neurol* 497:658–669.

McLaughlin T, Torborg CL, Feller MB, O’Leary DDM (2003) Retinotopic map refinement requires spontaneous retinal waves during a brief critical period of development. *Neuron* 40:1147–1160.

Mistretta CM, Labyak SE (1994) Maturation of neuron types in nucleus of solitary tract associated with functional convergence during development of taste circuits. *J Comp Neurol* 345:359–376.

Mrsic-Flogel TD (2005) Altered Map of Visual Space in the Superior Colliculus of Mice Lacking Early Retinal Waves. *J Neurosci* 25:6921–6928.

Nejad MS (1986) The neural activities of the greater superficial petrosal nerve of the rat in response to chemical stimulation of the palate. *Chem Senses* 11:283–293.

Ninomiya Y (1998) Reinnervation of cross-regenerated gustatory nerve fibers into

- amiloride-sensitive and amiloride-insensitive taste receptor cells. *Proc Natl Acad Sci U S A* 95:5347–5350.
- Ninomiya Y, Kajiura H, Mochizuki K (1993) Differential taste responses of mouse chorda tympani and glossopharyngeal nerves to sugars and amino acids. *Neurosci Lett* 163:197–200.
- Norgren R (1974) Gustatory afferents to ventral forebrain. *Brain Res* 81:285–295.
- Norgren R (1976) Taste pathways to hypothalamus and amygdala. *J Comp Neurol* 166:17–30.
- Norgren R, Leonard CM (1973) Ascending central gustatory pathways. *J Comp Neurol* 150:217–237.
- Pfaffmann C (1941) Gustatory Afferent Impulses. *J Cell Comp Physiol* 17:243–258.
- Pfeiffenberger C, Cutforth T, Woods G, Yamada J, Rene' R, Copenhagen D, Flanagan J, Feldheim D (2005) Ephrin-As and neural activity are required for eye-specific patterning during retinogeniculate mapping. *Nat Neurosci* 8:1022–1027.
- Renehan WE, Jin Z, Zhang X, Schweitzer L (1996) Structure and function of gustatory neurons in the nucleus of the solitary tract: II. Relationships between neuronal morphology and physiology. *J Comp Neurol* 367:205–221.
- Rosen AM, Di Lorenzo PM (2012) Neural coding of taste by simultaneously recorded cells in the nucleus of the solitary tract of the rat. *J Neurophysiol* 108:3301–3312.
- Shingai T, Beidler LM (1985) Response characteristics of three taste nerves in mice. *Brain Res* 335:245–249.
- Skyberg R, Sun C, Hill DL (2017) Maintenance of Mouse Gustatory Terminal Field

Organization is Disrupted Following Selective Removal of Peripheral Sodium Salt Taste Activity at Adulthood. *J Neurosci*.

Smith D V, Li CS, Davis BJ (1998) Excitatory and inhibitory modulation of taste responses in the hamster brainstem. *Ann N Y Acad Sci* 855:450–456.

Sollars SI, Hill DL (1998) Taste responses in the greater superficial petrosal nerve: substantial sodium salt and amiloride sensitivities demonstrated in two rat strains. *Behav Neurosci* 112:991–1000.

Sollars SI, Walker BR, Thaw a. K, Hill DL (2006) Age-related decrease of the chorda tympani nerve terminal field in the nucleus of the solitary tract is prevented by dietary sodium restriction during development. *Neuroscience* 137:1229–1236.

Spector AC, Glendinning JI (2009) Linking peripheral taste processes to behavior. *Curr Opin Neurobiol* 19:370–377.

Spector AC, Travers SP (2005) The representation of taste quality in the mammalian nervous system. *Behav Cogn Neurosci Rev* 4:143–191.

Stellwagen D, Shatz CJ (2002) An instructive role for retinal waves in the development of retinogeniculate connectivity. *Neuron* 33:357–367.

Sun C, Dayal A, Hill DL (2015) Expanded terminal fields of gustatory nerves accompany embryonic BDNF overexpression in mouse oral epithelia. *J Neurosci* 35:409–421.

Sun C, Hummler E, Hill DL (2017) Selective Deletion of Sodium Salt Taste During Development Leads to Expanded Terminal Fields of Gustatory Nerves in the Adult Mouse Nucleus of the Solitary Tract. *J Neurosci* 3:660–672.

Sweazey RD, Bradley RM (1989) Responses of neurons in the lamb nucleus tractus

- solitarius to stimulation of the caudal oral cavity and epiglottis with different stimulus modalities. *Brain Res* 480:133–150.
- Thompson A, Gribizis A, Chen C, Crair MC (2017) Activity-dependent development of visual receptive fields. *Curr Opin Neurobiol* 42:136–143.
- Tokita K, Boughter JD (2016) Topographic organizations of taste-responsive neurons in the parabrachial nucleus of C57BL/6J mice: An electrophysiological mapping study. *Neuroscience* 316:151–166.
- Tokita K, Inoue T, Boughter JD (2009) Afferent connections of the parabrachial nucleus in C57BL/6J mice. *Neuroscience* 161:475–488.
- Travers JB (1988) Efferent projections from the anterior nucleus of the solitary tract of the hamster. *Brain Res* 457:1–11.
- Travers SP (2002) Quinine and citric acid elicit distinctive Fos-like immunoreactivity in the rat nucleus of the solitary tract. *Am J Physiol Integr Comp Physiol* 282:R1798–R1810.
- Travers SP, Pfaffmann C, Norgren R (1986) Convergence of lingual and palatal gustatory neural activity in the nucleus of the solitary tract. *Brain Res* 365:305–320.
- Van Buskirk RL, Smith D V (1981) Taste sensitivity of hamster parabrachial pontine neurons. *J Neurophysiol* 45:144–171.
- Vogt MB, Hill DL (1993) Enduring alterations in neurophysiological taste responses after early dietary sodium deprivation. *J Neurophysiol* 69:832–841.
- Wang L, Bradley RM (1993) Influence of GABA on neurons of the gustatory zone of the rat nucleus of the solitary tract. *Brain Res* 616:144–153.

- Wang L, Bradley RM (1995) In vitro study of afferent synaptic transmission in the rostral gustatory zone of the rat nucleus of the solitary tract. *Brain Res* 702:188–198.
- Wang L, Liu M, Segraves MA, Cang J (2015) Visual Experience Is Required for the Development of Eye Movement Maps in the Mouse Superior Colliculus. *J Neurosci* 35:12281–12286.
- Wang L, Rangarajan K V., Lawhn-Heath CA, Sarnaik R, Wang B-S, Liu X, Cang J (2009) Direction-Specific Disruption of Subcortical Visual Behavior and Receptive Fields in Mice Lacking the 2 Subunit of Nicotinic Acetylcholine Receptor. *J Neurosci* 29:12909–12918.
- Whitehead M (1990) Subdivisions and Neuron Types of the Nucleus of the Solitary Tract That Project to the Parabrachial Nucleus in the Hamster. *J Comp Neurol* 574:554–574.
- Whitehead MC (1988) Neuronal architecture of the nucleus of the solitary tract in the hamster. *J Comp Neurol* 276:547–572.
- Whitehead MC (1993) Distribution of synapses on identified cell types in a gustatory subdivision of the nucleus of the solitary tract. *J Comp Neurol* 332:326–340.
- Whitehead MC, Bergula A, Holliday K (2000) Forebrain projections to the rostral nucleus of the solitary tract in the hamster. *J Comp Neurol* 422:429–447.
- Whitehead MC, McPheeters M, Savoy LD, Frank ME (1993) Morphological types of neurons located at taste-responsive sites in the solitary nucleus of the hamster. *Microsc Res Tech* 26:245–259.
- Whiteside B (1927) Nerve Overlap in the Gustatory Apparatus of the Rat. *J Comp Neurol*:363–377.

- Wiesel TN, Hubel DH (1963) Effects of Visual Deprivation on Morphology and Physiology of Cells in the Cats Lateral Geniculate Body. *J Neurophysiol* 26:978–993.
- Wolf G (1968) Projections of thalamic and cortical gustatory areas in the rat. *J Comp Neurol* 132:519–529.
- Yamamoto T, Kawamura Y (1975) Dual innervation of the foliate papillae of the rat: An electrophysiological study.
- Zheng S, Sun C, Hill DL (2014) Postnatal reorganization of primary gustatory afferent terminal fields in the mouse brainstem is altered by prenatal dietary sodium history. In: Society for Neurosciences.
- Ziburkus J, Guido W (2006) Loss of binocular responses and reduced retinal convergence during the period of retinogeniculate axon segregation. *J Neurophysiol* 96:2775–2784.

Figure 1

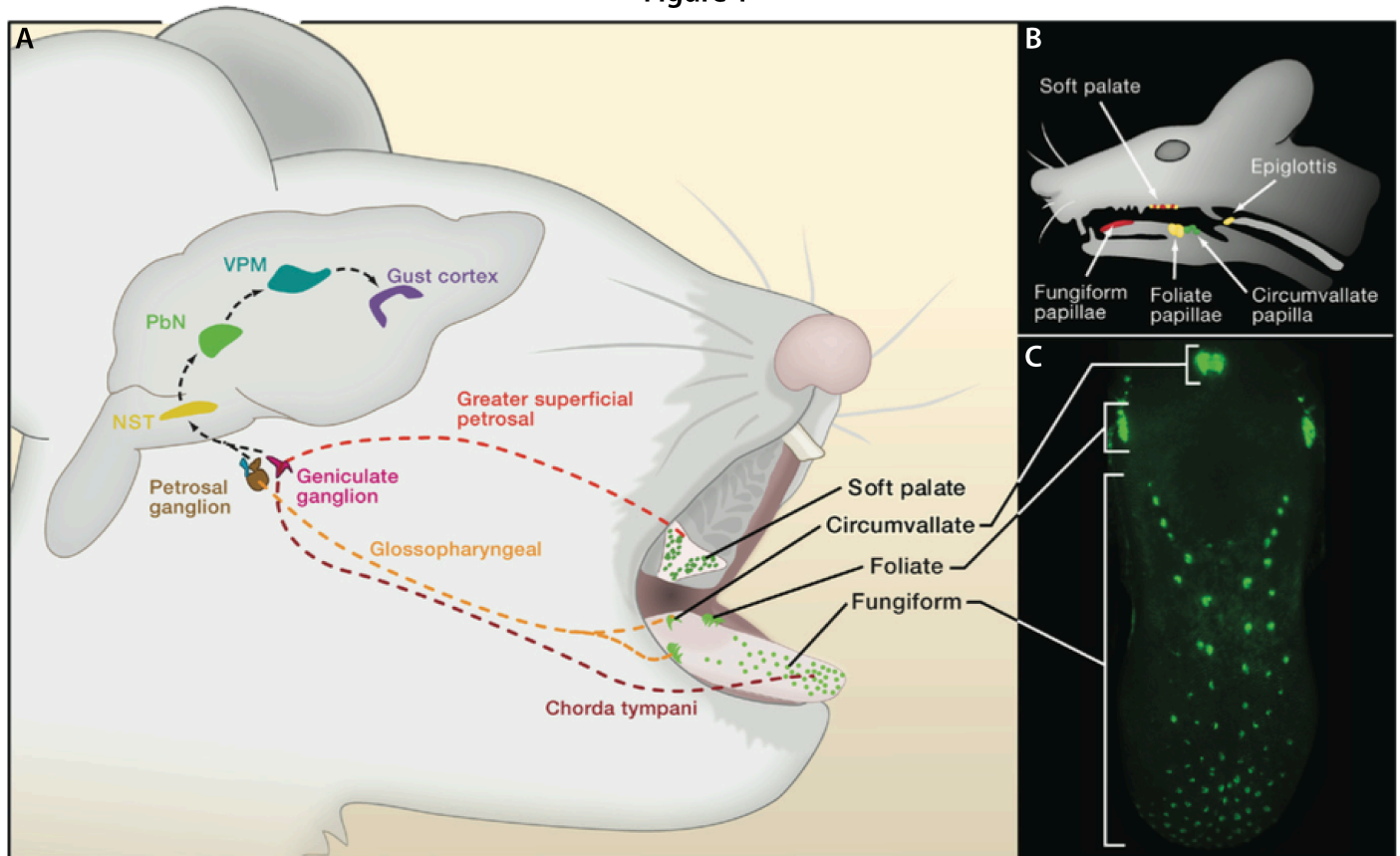


Figure 1: Gustatory system circuitry. **(A)** The chorda tympani (CT), greater superficial petrosal (GSP), and glossopharyngeal (IX) nerves carry taste related information from taste buds throughout the oral cavity to the nucleus of the solitary tract (NST). The CT innervates the anterior two thirds of the tongue, the IX innervates the posterior one third of the tongue, and the GSP innervates the soft palate and geschmacksstreifen (not shown) on the roof of the mouth. From the NST, taste responses are transmitted through the parabrachial nucleus (PbN) and thalamus (VPM) to the primary gustatory cortex in the insula. **(B)** Illustration depicting areas in the oral cavity that contain taste buds. **(B-C)** Fungiform papillae are distributed across the anterior two thirds of the tongue, foliate papillae are found on the lateral edge of the posterior one third of the tongue, and the circumvallate papilla is located at the very back of the tongue. **(C)** The organization of these three classes of papillae can be seen by genetically engineering mice to express green fluorescent protein in taste bud cells. Figure adapted from Yarmolinsky et al., 2009.

Figure 2

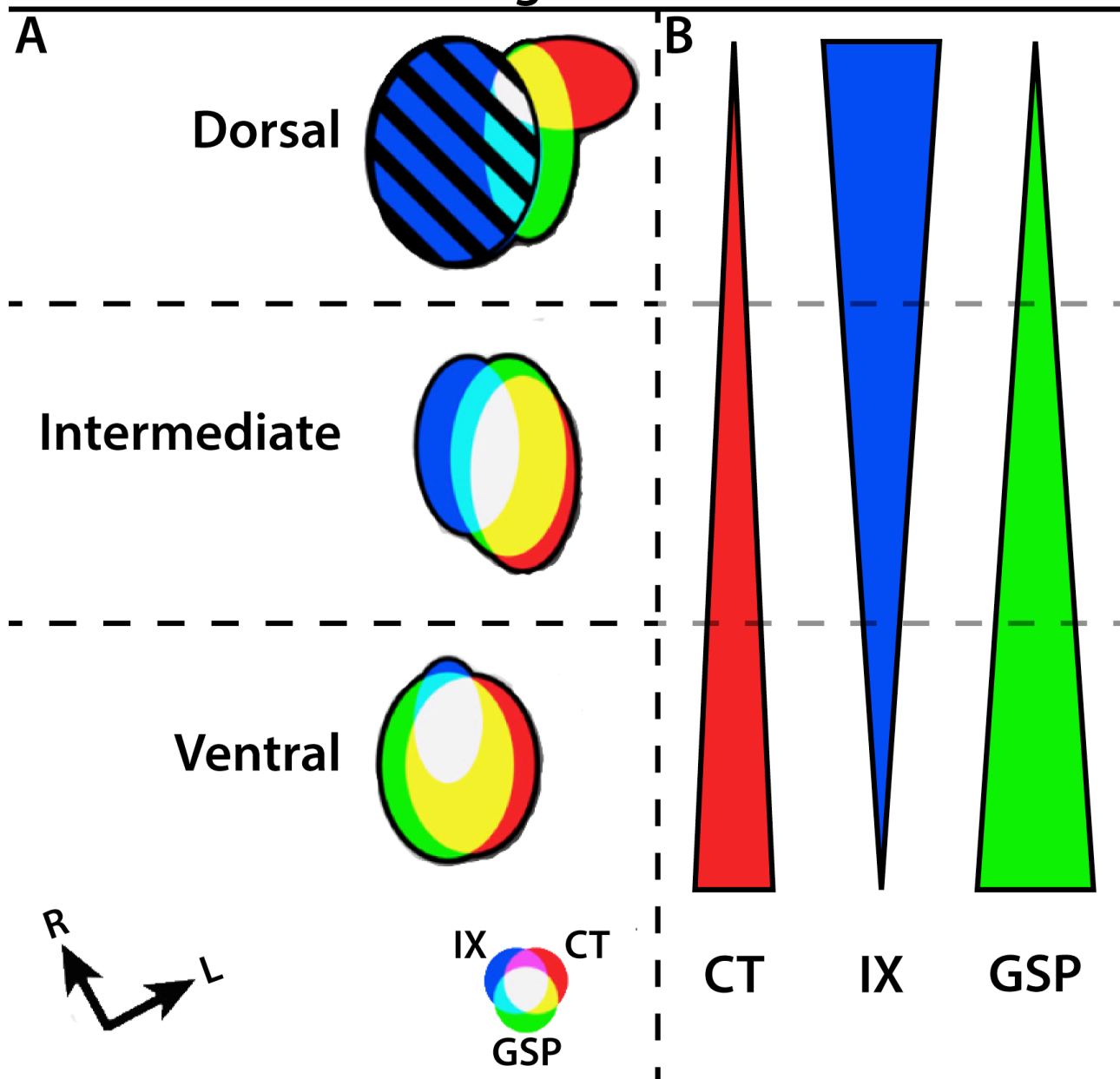


Figure 2: Schematic of the terminal field organization throughout the dorsal-ventral axis of the nucleus of the solitary tract (NST) in adult WT mice. **(A)** The size of each terminal field was calculated relative to the terminal field volume for the IX nerve (hatched blue oval in dorsal zone; area = 1.0). The color of individual nerves and their overlaps are shown in the color wheel. The orientation of the ovals are shown as they appear in horizontal sections. R, rostral; L, lateral. **(B)** Illustration summarizing the gross organization of each gustatory nerve terminal field throughout the dorsal ventral axis of the NST. Image adapted from Sun et al., 2015.

Figure 3

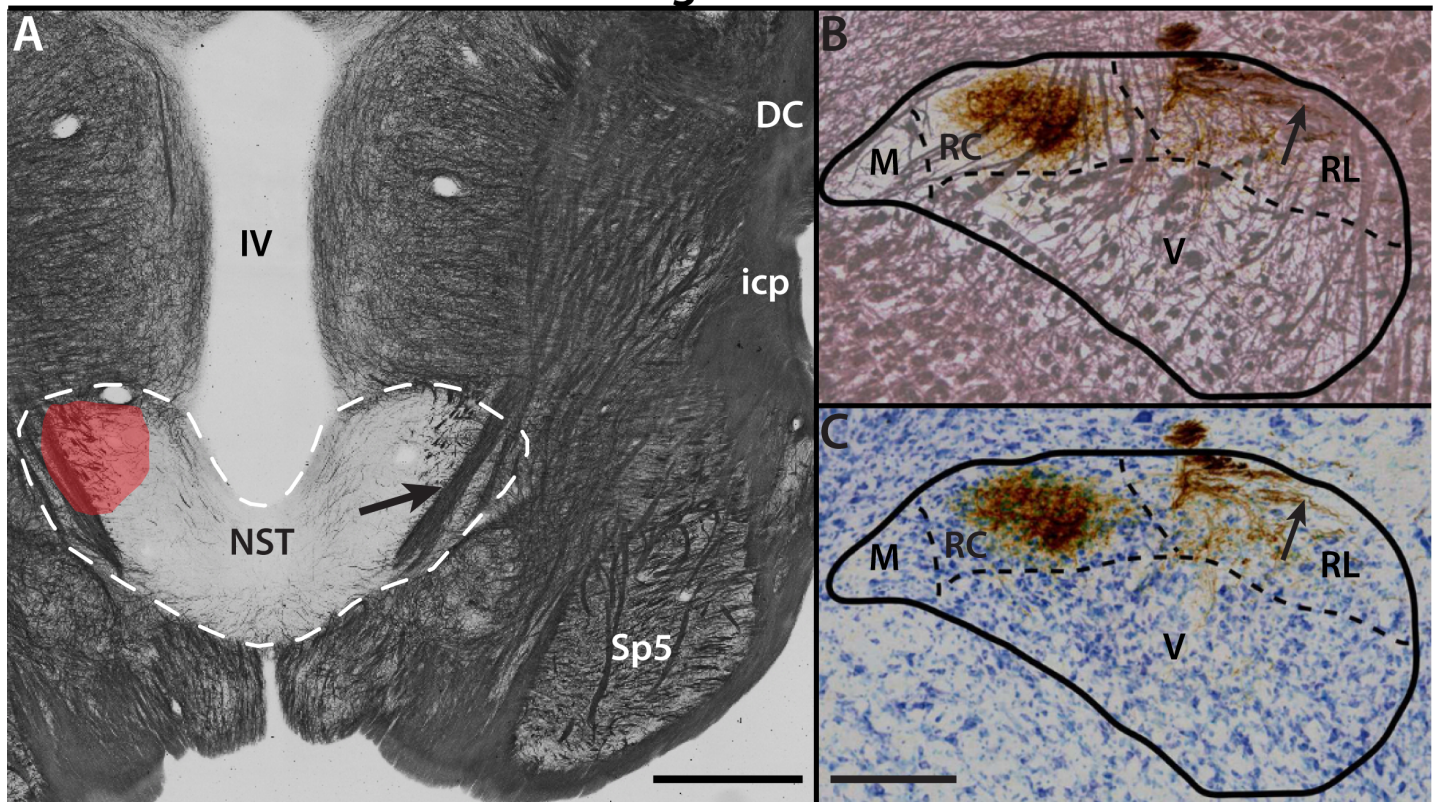


Figure 3: Anatomy of the nucleus of the solitary tract (NST). **(A)** Horizontal myelin-stained brainstem section. The border of the NST is marked with a dotted line and the arrows point to the solitary tract. The area mark by red in the left NST delineates where gustatory afferent nerve axons innervate the NST. IV, fourth ventricle; DC, dorsal cochlear nucleus; icp, inferior cerebellar peduncle; Sp5, spinal trigeminal nucleus; R, rostral; L, lateral. Scale bar in **A**, 500 μ m. **(B-C)** Coronal myelin-stained **(B)** and nissl-stained **(C)** brainstem sections. The borders of the NST are in black and subdivisions of the NST are marked by dotted lines. The arrows point to the solitary tract. Brown labeling in **B** and **C** is the chorda tympani terminal field. M, medial subdivision; RC, rostrocentral subdivision; RL, rostrolateral subdivision; V, ventral subdivision. Scale bar in **C**, 250 μ m and also applies to **B**. Image adapted from Corson et al., 2012.

Figure 4

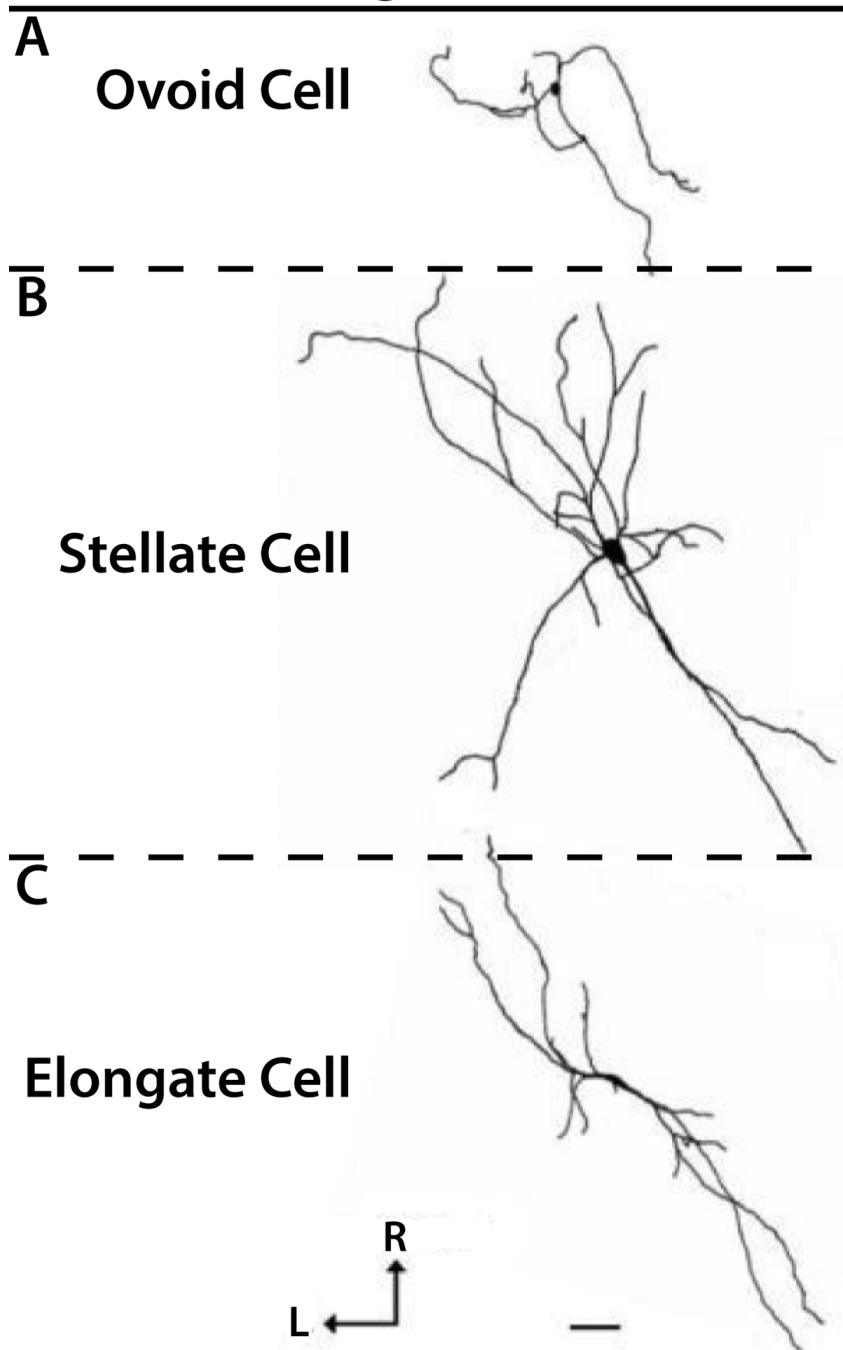


Figure 4: Cell types in the nucleus of the solitary tract. Biocytin-filled ovoid (A), stellate (B), and elongate (C) NST cells. R, rostral; L, lateral. Scale bar in C, 50 μ m. Image adapted from King et al., 1994.

Figure 5

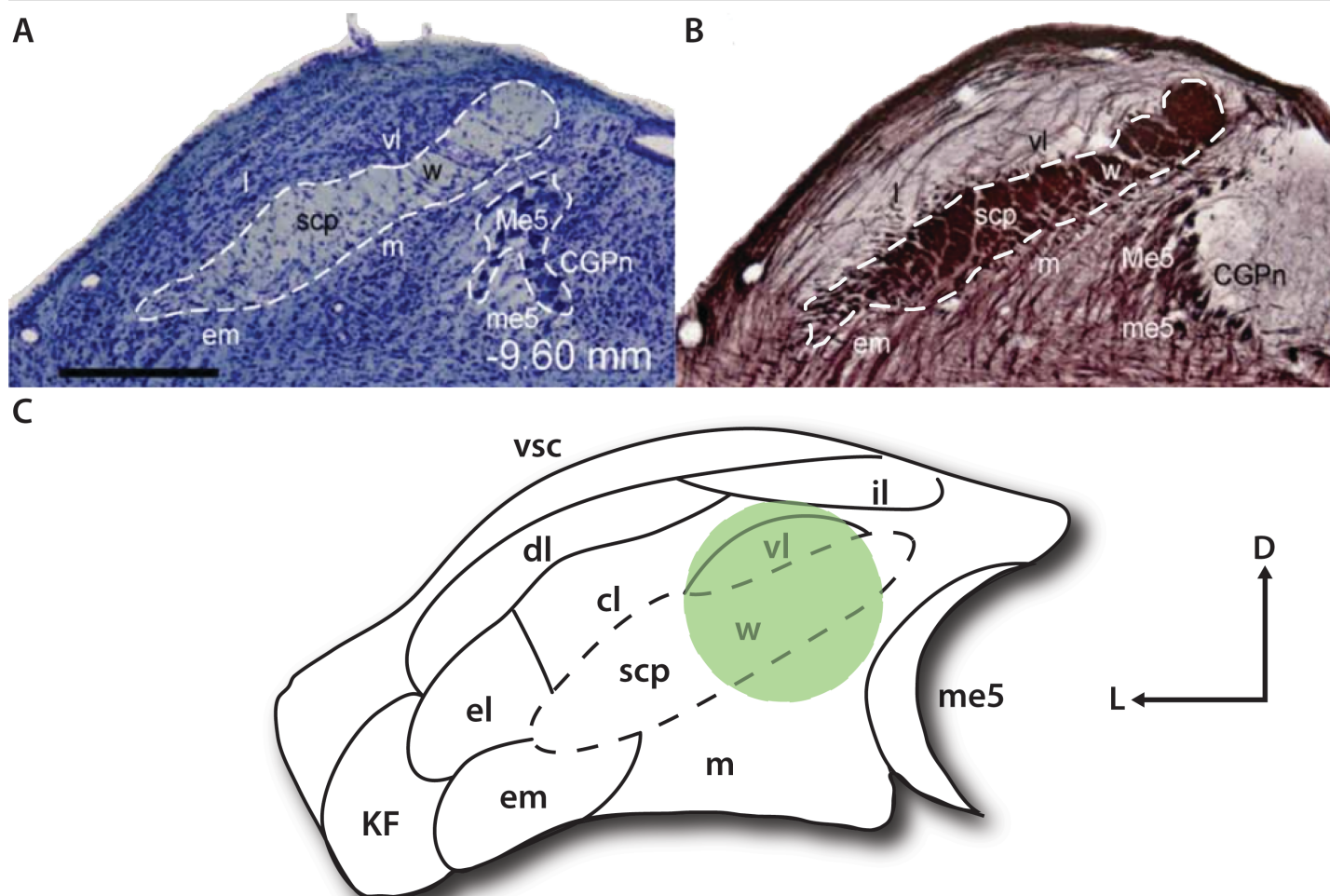


Figure 5: Anatomy of the parabrachial nucleus (PBN). **(A-B)** Nissl-stained **(A)** and myelin-stained **(B)** coronal sections of the PBN. The dotted white line demarcates the “waist” region of the PBN. The smaller section delineated with a dotted white line in **(A)** is the mesencephalic trigeminal nucleus (Me5). **(C)** Enlarged illustration depicting the subdivisions within the PBN. The black dotted line outlines the waist region of the PBN. The green area is the targeted injection site. l, lateral parabrachial nucleus; vl, ventral lateral parabrachial nucleus; em, external medial parabrachial nucleus; m, medial parabrachial nucleus; scp, superior cerebellar peduncle; w, waist region of the parabrachial nucleus; Me5, mesencephalic trigeminal nucleus; me5, mesencephalic trigeminal tract; CGPn, central gray of the pons; D, dorsal; L, lateral. Scale bar in **A**, 300 μ m. Image adapted from Holtz et al., 2015.

Figure 6

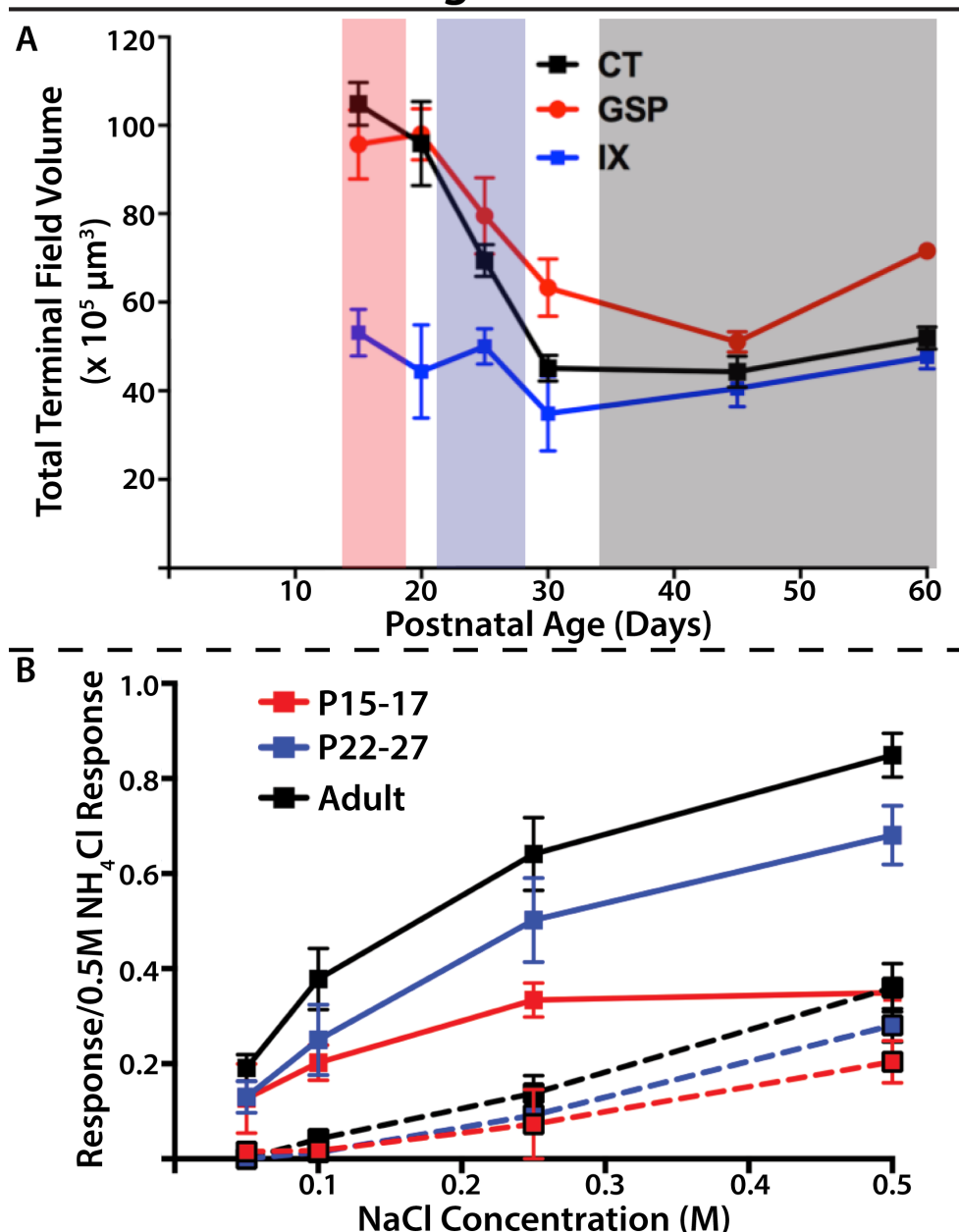


Figure 6: Development of the peripheral gustatory system. **(A)** Development of mouse gustatory afferent nerve terminal fields in the nucleus of the solitary tract (NST). Red, blue, and black shading corresponds to the age groups used in **B**. **(B)** Quantified whole nerve taste responses from the chorda tympani (CT) in WT mice to a concentration series of NaCl (0.05, 0.1, 0.25, and 0.5M) in mice aged P15-17 (red), P22-27 (blue), and adult (black). Responses were recorded before (whole lines) and after (dotted lines) lingual application of the ENaC blocker, amiloride. **(C)** Individual whole nerve taste responses from mice within the P22-27 age group show large variability in their responsiveness to NaCl stimulation. Responses were calculated as the response to each stimulus presented relative to the 0.5M NH₄Cl responses to account for variation in the whole nerve preparation.

Selective Removal of Sodium Salt Taste Disrupts the Maintenance of Dendritic Architecture of Second Order Taste Neurons in the Mouse Nucleus of the Solitary Tract

Rolf Skyberg, Chengsan Sun, David L. Hill
Department of Psychology
PO Box 400400, University of Virginia,
Charlottesville, VA 22904-4400

Abbreviated Title: Taste Activity Maintains Dendritic Architecture

Corresponding Author: Dr. David L. Hill
Department of Psychology
PO Box 400400
University of Virginia
Charlottesville, VA 22904
dh2t@virginia.edu
telephone: (434) 982-4728
fax: (434) 982-4785

Number of Pages: 47

Number of Figures: 10

Number of Tables: 0

Number of Words: Abstract – 248
Significance – 120
Introduction – 902
Discussion – 2364

Conflict of Interest: The authors declare no competing financial interests.

Acknowledgements: This work was supported by National Institute of Health Grant DC00407 (to DLH).

Abstract

Neuronal activity plays critical roles in the development of sensory circuits in the mammalian brain. Recently, experimental manipulations have become available to alter gustatory activity from specific taste transduction pathways to investigate the roles taste experience play in the development of central gustatory circuits. Here we used a previously vetted mouse knockout model in which the transduction channel necessary for sodium taste is removed from taste bud cells throughout life. In these knockout mice, the terminal fields that carry taste information from the periphery into the nucleus of the solitary tract (NST) fail to develop, suggesting that neural sodium taste activity is important for the proper development of central gustatory circuits. Using this model, we tested the hypothesis that the development and maintenance of the dendritic architecture of NST relay cells, the primary postsynaptic partner of gustatory nerve terminal fields, are similarly dependent upon sodium taste activity from this single transduction pathway. The dendritic fields of NST relay cells, from adult male and female mice in which the α -subunit of the epithelial sodium channel was conditionally deleted in taste bud cells (α ENaC knockout mice) throughout life, were up to 2.4x larger and more complex than that of age-matched control mice. Interestingly, these differences in dendritic architecture were not present in postnatal day 20 (P20) mice of either sex. Overall, our results suggest that ENaC-mediated sodium taste activity is necessary for the maintenance of dendritic fields of relay cells in the gustatory NST.

Significance Statement

Neural activity plays major roles in the development of sensory circuits in the mammalian brain. Here, we tested if the loss of sodium taste activity throughout development impacts the development of the dendritic organization of relay cells in the first central gustatory relay, the nucleus of the solitary tract (NST). We found that, like the development of gustatory afferent terminal fields in the NST, the dendritic fields of relay cells in the NST also depend on sodium-elicited taste activity. However, the effects of our manipulation were not present in young mice, suggesting a novel role for sodium taste activity in the maintenance of NST relay cell dendritic architecture, and highlights a level of plasticity not seen in other sensory systems.

Introduction

Neuronal activity plays important roles in the development of sensory circuits in the mammalian brain (Brunjes, 1994; Cang et al., 2005; Lee et al., 2005; Leake et al., 2006; Guido, 2008; Sun et al., 2017). Both cortical and subcortical sensory circuits exhibit some level of activity dependence for proper development to occur. For example, visual circuits in the dorsal Lateral Geniculate Nucleus (dLGN) are shaped by spontaneous- and visually-evoked retinal activity (Katz and Shatz, 1996; Hooks and Chen, 2006; Guido, 2008). Removal of this retinal activity prevents the normal developmental pruning of terminal fields of retinal ganglion cells in the dLGN (Katz and Shatz, 1996; Hooks and Chen, 2006), alters the morphology of postsynaptic thalamocortical relay cells (Matthews et al., 1960; Wiesel and Hubel, 1963; Guillery, 1973; Friedlander et al., 1982), and inhibits the

refinement of synapses between retinogeniculate afferents and thalamocortical relay cells (Stellwagen and Shatz, 2002; Jaubert-Miazza et al., 2005; Butts et al., 2007; Hooks and Chen, 2008; El-Danaf et al., 2015; Thompson et al., 2017). Thus, retinal activity impacts multiple cellular sites in developing central visual pathways.

By comparison, less is known about the roles neural activity plays in the development of subcortical gustatory circuits – areas that regulate feeding and motivated behaviors (Spector and Travers, 2005; Spector and Glendinning, 2009). Moreover, a few of the developmental characteristics observed in other sensory systems occur in the gustatory system. For instance, the three gustatory nerves that carry taste-related neural activity from the oral cavity into the medulla depend on neural activity to drive their anatomical development (Sun et al., 2017). The terminal fields of the chorda tympani (CT), greater superficial petrosal (GSP) and glossopharyngeal (IX) nerves innervate the nucleus of the solitary tract (NST) in the brainstem, where they initially create large, overlapping terminal fields (Mangold and Hill, 2008; Zheng et al., 2014). Throughout postnatal development, these terminal fields are “pruned” back into a smaller, more segregated, mature organization (Sollars et al., 2006; Mangold and Hill, 2008; Zheng et al., 2014). Interestingly, these dramatic changes occur during a period in which sodium taste activity, mediated via the epithelial sodium channel (ENaC), undergoes a twofold increase in magnitude, suggesting increases in peripheral input from this single transduction pathway may be driving the development of terminal fields in the NST (Hill & Bour, 1985; Zheng et al., 2014). By genetically removing functional ENaCs in taste bud cells throughout pre- and postnatal development, Sun et al., (2017)

demonstrated that sodium salt elicited activity was, in fact, necessary for the development of gustatory terminal fields in the NST. Adult α ENaC KO mice lacking functional ENaCs had significantly diminished CT and GSP whole nerve responses to a concentration series of NaCl (Skyberg et al., 2017; Sun et al., 2017) and did not exhibit normal appetitive licking behaviors to NaCl (Chandrashekar et al., 2010). Importantly, the CT, GSP, and IX nerve terminal fields in these knockout mice were roughly 2x larger than age matched controls at adulthood and were more reminiscent of immature control mice terminal fields (Sun et al., 2017). Similarly, the maintenance of these terminal fields in a mature state is also dependent upon normal levels of ENaC-mediated sodium taste activity, without which terminal fields revert back to an immature organization (Skyberg et al., 2017). Thus, sodium salt taste from this single transduction pathway plays multiple roles in the proper organization of gustatory terminal fields in the NST throughout an animal's life. These findings make this knockout mouse a unique and invaluable experimental model to answer questions regarding the roles of specific taste-elicited neural activity in the development, maintenance, and plasticity of other parts of the gustatory circuit.

While it is clear that sodium salt taste activity regulates both the development and maintenance of gustatory afferent terminal fields, it is not known if neural activity mediates the development of postsynaptic targets in the NST. Gustatory terminal fields in the NST predominantly synapse onto the dendrites of NST relay cells, which then send direct projections to the parabrachial nucleus (PBN) in the pons (Whitehead, 1990; Wang et al., 2012). These NST relay cells are

the location of the first central synapse in the gustatory pathway, and therefore are highly involved in the processing and decoding of gustatory activity. Despite this, little is known about the anatomical development of these relay cells. Here we test the hypothesis that the development and organization of these cells depends on proper levels of sodium salt taste activity, similar to that shown to occur with the development and maintenance of the presynaptic gustatory nerve terminal fields (Skyberg et al., 2017; Sun et al., 2017). Our results suggest that the dendritic architecture of NST relay cells in normally-developing mice reach a mature organization as early as P20. Given that ENaC-mediated sodium salt taste activity from the peripheral gustatory system is just beginning to develop by P20, it is unlikely that taste activity from this specific transduction pathway drives dendritic development of NST relay cells. However, the findings presented here indicate that, while ENaC-mediated sodium salt taste activity does not regulate NST relay cell dendritic development, it is required to maintain their dendritic organization into adulthood. Therefore, activity from a single taste modality (salty) is critical for the development and maintenance of presynaptic gustatory terminal fields and postsynaptic relay cell dendritic fields in the NST.

Materials and Methods

Animals

All experiments were approved by the University of Virginia Animal Care and Use Committee and followed guidelines set forth by the National Institutes of Health and the Society for Neurosciences. To examine the role of sodium salt taste on the development and organization of relay cell dendrites in the rostral NST, we used

mice described in detail by Chandrasekhar et al., 2010. Briefly, the alpha subunit of the epithelial sodium channel (α ENaC) was conditionally deleted in taste bud cells by crossing mice that drove the expression of Cre-recombinase under the cytokeratin 19 (CreK19) promoter with mice that were homozygous for the floxed *Scnn1a* (α ENaC) gene (*Scnn1a^{flox/flox}*). The CreK19 mice were generously supplied by Dr. Charles Zuker, and Dr. Edith Hummler supplied the *Scnn1a^{flox/flox}* mice. Therefore, our experimental animals had the genotype K19-Cre *Scnn1a^{flox/flox}* (α ENaC KO). The control group consisted of mice that were littermates to experimental animals, but did not have the CreK19 promoter (*Scnn1a^{flox/flox}*). To investigate the development of dendritic architecture, we retrogradely labeled relay cells in the NST at two significant developmental ages. First, we labeled NST relay cells in control and α ENaC KO mice between postnatal days 18-22 (P20 Controls, 4 mice, 2 male/2 female, 22 cells; P20 α ENaC KO, 3 mice, 2 male/1 female, 31 cells). We chose this age group for three reasons. First, at this age taste responses to NaCl have not fully matured (Fig 9; Hill & Bour, 1985; Zheng et al., 2014), allowing us to assess how dendritic architecture looks before peripheral taste input to the NST has fully matured. Second, the terminal fields of gustatory nerves in the NST begin their developmental “pruning” around this time, suggesting this to be a period of substantial functional and structural reorganization within the NST (Fig 8; Sollars et al., 2006; Mangold and Hill, 2008; Zheng et al., 2014). And finally, animals younger than P18 were too small to reliably fit into the stereotaxic device, making consistent targeting of the parabrachial nucleus (PBN) difficult. We also labeled NST relay cells in control and α ENaC KO mice between 60 – 120 days of age (Adult Control, 8 mice,

3 male/5 female, 123 cells; Adult α ENaC KO, 10 mice, 4 male/6 female, 81 cells). At these ages, both the peripheral taste responses and gustatory terminal fields in the NST have fully matured in control mice (Sollars et al., 2006; Mangold and Hill, 2008; Zheng et al., 2014). There were no sex-related differences found in any of our experiments or analyses, therefore male and female mice from the same experimental group were combined.

Parabrachial Nucleus Injections

Mice were sedated with a 0.32 mg/kg (0.24 mg/kg for P20 mice) injection of Domitor® (medetomidine hydrochloride: Pfizer Animal Health, Exton, PA; I.M.) and anesthetized with 40 mg/kg (30 mg/kg for P20 mice) Ketaset® (ketamine hydrochloride: Fort Dodge Animal Health, Fort Dodge, IA; I.M.). A water-circulating heating pad was used to maintain body temperature. Mice were placed in a non-traumatic head holder (Erickson, 1966) and an incision was made along the midline of the top of the head to expose the animal's skull. Bregma and lambda were then aligned horizontally and two 2x2mm holes were drilled in the skull approximately 5.2mm (5.1mm for P20 mice) caudal to bregma and 1.2mm (1.1mm for P20 mice) lateral to the midline, bilaterally (similar to Tokita et al., 2009; Tokita and Boughter, 2016). A glass pipette filled with 10% 3kD biotinylated dextran amine (BDA; Invitrogen, Carlsbad, CA; D7135) in 0.1M Citrate/NaOH buffer (pH 3.0) was slowly lowered 2.8mm (2.7mm for P20 mice) from the top of the cerebellum. This acidic solvent increased retrograde axonal uptake of the tracer and provided Golgi-like cell labeling in the NST (Kaneko et al., 1996; Reiner et al., 2000; Corson and Erisir, 2013). BDA was injected iontophoretically with a 6 μ A positive current (7s on, 7s

off) for 10min (Reiner et al., 2000; Fekete et al., 2015). Following the injection, the pipette tip was left in place without any positive current for 5 minutes to allow time for tracer uptake and to reduce backflow of tracer through the injection site. The pipette was then slowly raised out of the brain and the procedure was repeated on the other side of the brain, resulting in bilateral PBN injections. The animal's scalp was then sutured or sealed using Vetbond™ and the animal was injected with 5 mg/ml (3.75mg/ml for P20 mice) Antisedan® (atipamezole hydrochloride: Pfizer Animal Health, Exton, PA; I.M) to promote reversal of anesthesia.

Chorda Tympani Nerve Label

Procedures used to label the chorda tympani (CT) terminal field with fluorescent tracers were similar to that described previously in mouse (Sun et al., 2015, 2017; Skyberg et al., 2017). Briefly, 24-hours after PBN injections, animals were anesthetized as described above, placed into a non-traumatic head holder (Erickson, 1966), and maintained at 36°C with a water-circulating heating pad. The animal was placed into the supine position and an incision was made along the ventral midline of the neck. Musculature was retracted to expose the right tympanic bulla. The bulla was opened and the CT was cut peripheral to the geniculate ganglia. Crystals of 3kD tetramethylrhodamine dextran amine (TMR; Thermofisher Scientific, Waltham, MA; D3308, RRID: AB_2315472) were placed on the central stump of the CT, and the opening of the bulla was filled with Kwik-Sil (World Precision Instruments, Inc.; Sarasota, FL) to prevent crystals from diffusing from the site of the intended label. The incision was then sutured and the animal was revived using

Antisedan® (atipamezole hydrochloride: Pfizer Animal Health, Exton, PA; I.M) as described above.

Tissue Preparation

Following a 48-hour survival period, animals were deeply anesthetized with urethane and transcardially perfused with Krebs-Henseleit buffer (pH 7.3), followed by 4% paraformaldehyde (pH 7.2). Brains were removed, postfixed in 4% paraformaldehyde overnight, and then sectioned horizontally on a vibratome at 100 μ m. We chose to section tissue in the horizontal plane, as the dendritic arbors run parallel to this plane of sectioning, thus reducing the number times we transected dendrites. It is also the plane in which the gustatory afferent axons branch from the solitary tract and project primarily medially in rodents (Davis and Jang, 1988; Whitehead, 1988; Lasiter et al., 1989). Sections were then incubated in PBS containing 0.4% Triton for 1 hour. They were then placed in PBS containing 0.2% Triton with 1:400 streptavidin Alexa Fluor 488 (Jackson ImmunoResearch Labs, Inc., West Grove, PA; 016-540-084, RRID: AB_2315383) for 2 hours to visualize the biotinylated dextran amine filled NST relay cells. The CT terminal fields were labeled with TMR and did not require further processing for visualization. Sections were mounted onto gel-coated slides and coverslipped with Vectashield Hard Mounting Medium (Vector Laboratories, Burlingame, CA).

To verify our stereotaxic injection parameters 1 mouse from each group was injected and processed as described above. However, these brains were sectioned coronally at 100 μ m to allow for viewing of the injection tract as well as the center of the injection (Fig 1A).

Confocal Microscopy

Tissue was imaged using a Nikon 80i microscope fitted with a Nikon C2 scanning system (Nikon Instruments, INC., Melville, NY). NST relay cells were located and imaged using a 10x objective (Nikon, CFIPlanApo; NA=0.45) followed by a higher resolution image taken with a 63x oil-immersion objective (Nikon, PlanApo VC; NA=1.4). The fluorescent labels used were matched for the wavelengths of two of the three lasers in the system (argon laser – 488nm, 10mW, NST relay cells; DPSS laser – 561nm, 10mW, CT). Sequential optical sections were captured every 1 μ m through the extent of every imaged cell. Images were obtained with settings adjusted so that pixel intensities were near (but not at) saturation.

Data Analysis

Confocal images were imported into NeuroLucida 11.11.12 (MBF Bioscience, Williston, VT, USA; RRID:SCR_001775) and reconstructions were made by tracing the dendritic architecture and cell bodies throughout the z-stack. These tracings were then opened in NeuroLucida Explorer 2.7 (MBF Bioscience, Williston, VT, USA; RRID:SCR_001775) and measures were taken on the dendritic architecture of each retrogradely-filled NST relay cell tracing. These measures included: the number of primary dendrites, number of dendritic branch points, number of dendritic endings, dendritic length, mean dendritic length, and the dendritic complexity index (DCI). The DCI was determined from the following equation, $DCI = (\text{sum of branch tip order} + \text{number of dendritic endings}) * (\text{total dendritic length} / \text{number of primary dendrites})$ (Pillai et al., 2012).

In addition to collecting basic measures of dendritic architecture we also performed Sholl analyses (Sholl, 1956) on each of the traced NST-relay cells using NeuroLucida Explorer 2.7 (MBF Bioscience, Williston, VT, USA; RRID:SCR_001775). A series of concentric rings were placed over the traced neuron, centered on the cell body. The centermost ring had a diameter of 20 μ m while each of the concentric rings successively increased their diameter by 5 μ m.

Finally, we also calculated a polar histogram for each traced cell using NeuroLucida Explorer 2.7 (MBF Bioscience, Williston, VT, USA; RRID:SCR_001775). This technique displays the length and direction of dendritic processes in a two-dimensional format. These polar histograms show the total length of dendrites present within 20° bins, covering 360° in the horizontal plane. To normalize the angle that horizontal brain sections were mounted onto slides, a straight line was drawn from the bottom to the top of the fourth ventricle (or along the midline whenever the ventricle was not present). Representative tracings were then rotated as needed until the drawn line was oriented vertically. Then, we reflected all cells from the left NST 180° horizontally (that is along the rostral-caudal axis of the brain). The resulting data sets are a collection of cells from the left and the right NST.

Analysis of Relay Cells along the Dorsal-Ventral Axis of the NST

To assess and compare the distributions of relay cells within the NST we recorded and plotted the location of a majority of the retrogradely-filled relay cells (231 of 257) onto representative horizontal brainstem tracings. The location of 26 relay cells were not able to be reliably calculated due to significant degradation of

the tissue. To be consistent with previous literature, cells were grouped into four zones based on the dorsal-ventral axis of the NST they were located. The landmarks used to define these four zones were similar to what has been reported previously in mouse (Sun et al., 2015, 2017; Skyberg et al., 2017) and rat (King and Hill, 1991; Krimm and Hill, 1997; May and Hill, 2006; Sollars et al., 2006; Mangold and Hill, 2008; Corson and Hill, 2011). The first zone, the far dorsal zone of the NST, is characterized by sections with a relatively large fourth ventricle, a small solitary tract in the rostral portion of the NST, and by a lack of the hypoglossal and facial nucleus. The far dorsal zone is located between 100 μ m and 300 μ m from the top of the brainstem in mouse (Fig 3). The dorsal zone also contains the fourth ventricle but, in these sections, it does not extend as far in the medial-lateral plane. Sections from the dorsal zone have an NST that extends more rostrally than in the far dorsal zone, a solitary tract that occupies nearly the entire rostral-caudal extent of the NST, and the presence of the dorsal cochlear nucleus. The dorsal zone is just dorsal to the hypoglossal nucleus and is located roughly 300 μ m to 500 μ m from the top to the brainstem (Fig 3). The intermediate zone is characterized by a significant thinning of the fourth ventricle compared to the far dorsal and dorsal zones, the solitary tract is thinner and shorter than seen in the dorsal zone, the rostral pole of the NST extends further anteriorly than in the dorsal zone, and both the hypoglossal and facial nuclei are evident. The intermediate zone is located around 500 μ m and 800 μ m from the top of the brainstem (Fig 3). The ventral zone is at the level ventral to the fourth ventricle, the NST is less defined and narrow at its rostral extent, the ventral cochlear nucleus is apparent, and the hypoglossal and facial nuclei are

evident. The ventral zone contains the remainder of the NST and is located roughly 800 μ m and 1200 μ m from the top of the brainstem (Fig 3). It should be noted that the NST is oriented within the brainstem with the caudal-most portion of the NST positioned dorsal to the rostral-most portion of the NST (Ganchrow et al., 2014). That is, the NST extends ventrally and rostrally from the caudal-most extent of the NST. Therefore, the far dorsal zone more accurately represents the dorsal-caudal portion of the NST and the ventral zone represents the more ventral-rostral portion of the NST.

Chorda Tympani Nerve Neurophysiology

To establish that the knockout of the *Scnn1a* gene in the tongue resulted in reduced functional CT responses to NaCl and to determine the normal development of ENaC function in control mice, we recorded taste-stimulus-evoked whole nerve activity from the CT from each group of mice using methods described previously (Sun et al., 2015, 2017; Skyberg et al., 2017). Briefly, mice were anesthetized as described for the retrograde parabrachial injection procedure. The animals were then tracheotomized and placed on a circulating water heating pad to maintain body temperature. Hypoglossal nerves were transected bilaterally to prevent tongue movement, and the mouse was placed in a nontraumatic head holder. The left CT nerve was isolated using a mandibular approach. The nerve was exposed near the tympanic bulla, cut, desheathed, and positioned on a platinum electrode. A second electrode was placed in nearby muscle to serve as a reference. Kwik-Sil (World Precision Instruments, Inc.; Sarasota, FL) was placed in the cavity around the nerve to maintain the preparation.

Stimulation Procedure

All chemicals were reagent grade and prepared in artificial saliva (Hellekant et al., 1985). Neural responses from the CT were recorded to ascending concentrations series of 0.05, 0.1, 0.25, and 0.5 M NaCl, to 10, 20, to assess the taste responses to prototypical stimuli that represent salty to humans. Each concentration series was bracketed by applications of 0.5M NH₄Cl to monitor the stability of each preparation and for normalizing taste responses. Solutions were applied to the tongue in 5 ml aliquots with a syringe and allowed to remain on the tongue for ~20 sec. We used this period of stimulation so that we could ensure enough of a period to measure the steady state responses. After the application of each solution, the tongue was rinsed with artificial saliva for ≥ 1 min (Hellekant et al., 1985). This period allowed a full recovery of neural responses (i.e., the responses were not adapted by previous responses) (Shingai and Beidler, 1985). In addition, responses were recorded to the NaCl concentration series in presence of the epithelial sodium channel blocker, amiloride (50 μ M). Rinses during this series were with amiloride in artificial saliva.

All responses were calculated as follows: the average voltage of the spontaneous activity that occurred for the second before stimulus onset was subtracted from the voltage that occurred from the period from the first to sixth second after stimulus application. Response magnitudes were then expressed as ratios relative to the mean of 0.5M NH₄Cl responses before and after taste stimulation. Whole nerve response data were retained for analysis only when 0.5M NH₄Cl responses that bracketed a concentration series varied by <10%.

Experimental Design and Statistical Analyses

All measurements presented are given as mean (\pm SEM). Prism 7 (GraphPad; RRID:SCR_002798) was used for quantification and statistical analyses.

Measurements of NST Relay Cell Location and Dendritic Morphology

Experiments investigating NST relay cell dendritic architecture were conducted in control and α ENaC KO mice at P18-22 (P20 Control, 4 mice, 2 male/2 female; P20 α ENaC KO, 3 mice, 2 male/1 female) and P60-120 (Adult Control, 8 mice, 3 male/5 female; Adult α ENaC KO, 10 mice, 4 male/6 female). We collected and analyzed 22 cells from P20 control mice, 31 cells from P20 α ENaC KO mice, 123 cells from adult control mice, and 81 cells from adult α ENaC KO mice. The χ^2 test was used to compare the proportion of bipolar and multipolar cells in both animal groups at each age as well as to compare the distribution of relay cells along the dorsal-ventral axis of the NST between control and α ENaC KO mice at both ages. A one-way ANOVA was used to statistically compare measures of dendritic architecture (number of primary dendrites, number of dendritic branches, total dendritic length, dendritic complexity) between control and α ENaC KO mice at P20 and adulthood. To statistically compare the frequency, length, and mean length of each order of dendrite between control and α ENaC KO mice at P20 and adulthood a two-way ANOVA was used (4 groups X 7 dendritic orders). Two-way ANOVAs were also used to compare measurements collected from sholl analyses of cells from control and α ENaC KO mice at P20 and adulthood (4 group X 47 distances from cell soma). We used the Bonferroni procedure to account for multiple comparisons (Armstrong, 2014) and considered p values ≤ 0.05 to be significant. The mean (\pm

SEM) values for each measure (i.e. dendritic length) were compared across all four groups.

Total Chorda Tympani Terminal Field Volumes

Experiments inspecting the total chorda tympani terminal field volume were done in control and α ENaC KO mice at P20 (P20 Control, 6 mice, 3 male/3 female; P20 α ENaC KO, 3 mice, 3 male/0 female) and P60-120 (Adult Control, 7 mice, 3 male/4 female; Adult α ENaC KO, 6 mice, 4 male/2 female). The mean (\pm SEM) total CT terminal field volume was calculated for control and α ENaC KO mice at P20 and adulthood, and a one-way ANOVA was used to statistically compare these means. The Bonferroni procedure was used to account for multiple comparisons (Armstrong, 2014) and only p values ≤ 0.05 were considered to be significant.

Chorda Tympani Whole Nerve Neurophysiology

Experiments examining chorda tympani whole nerve neurophysiology were done in control and α ENaC KO mice at P20 (P20 Control, 3 mice, 2 male/1 female; P20 α ENaC KO, 2 mice, 1 male/1 female) and P60-120 (Adult Control, 5 mice, 3 male/2 female; Adult α ENaC KO, 3 mice, 1 male/2 female). A two-way ANOVA was used to compare mean (\pm SEM) relative CT responses (normalized to 0.5M NH_4Cl responses) between P20 control, P20 ENaC KO, adult control, and adult ENaC KO mice to a concentration series of NaCl (4 groups X 4 concentrations). The Bonferroni procedure was used to correct form multiple comparisons (Armstrong, 2014). We considered p values ≤ 0.05 to be significant.

Results

BDA injections into the “waist” region of the PBN resulted in Golgi-like, retrograde labeling of relay cells in the NST (Fig 1). For the relay cells from the P20 control mice (n=22), only 2 cells (9.10%) were bipolar (elongate) while 20 (90.9%) were multipolar (fusiform). Similarly, of the 123 relay cell from adult control mice, only 16 (13.0%) were bipolar while 107 cells (87.0%) were multipolar. The P20 α ENaC KO and adult α ENaC KO relay cell populations had similar proportions of bipolar and multipolar cells as the control populations. For the relay cells from P20 α ENaC KO mice (n=31), 3 cells (9.70%) were bipolar while 28 cells (90.3%) were multipolar. Of the 81 relay cells from α ENaC KO mice, 6 (7.40%) were bipolar and the remaining 75 (92.6%) were multipolar. Statistical analysis confirmed that the distribution of bipolar and multipolar cells in all four groups were not statistically different from each other ($X^2(3) = 1.72, p=0.634$). These distributions were comparable to what has been reported in another study of rodent NST relay cell morphology (Corson and Erisir, 2013). See figure 2 for representative cell tracings from P20 control (Fig 2A), adult control (Fig 2B), P20 α ENaC KO (Fig 2C), and adult α ENaC KO mice (Fig 2D).

Distribution of Relay Cells Within the NST Along the Dorsal-Ventral Axis

Figure 3 shows the location of 231 of the 257 retrogradely-labeled relay cells in the NST. Relay cells were located throughout the dorsal ventral axis of the NST. About 37 (16.0%) cells, regardless of condition, were located in the far dorsal zone of the NST. The dorsal and intermediate zones contained a large majority of retrogradely-labeled relay cells, 77 (33.3%) cells and 98 (42.4%) cells, respectively. Finally, the ventral zone only contained 19 (8.30%) retrogradely-labeled cells.

The dorsal-ventral distribution of relay cells from adult control mice were not statistically significant different than that of adult ENaC KO mice ($X^2 (3) = 7.44$, $p=0.06$). Thus, the two adult populations of relay cells were not sampled differently along the dorsal-ventral axis. However, when we compared the dorsal-ventral distribution of relay cells from the P20 control population with that of the adult control distribution we found a statistically significant difference ($X^2 (3) = 9.89$, $p=0.02$). The distribution of relay cells from P20 control mice was shifted towards the far dorsal (27.0% in P20 controls vs 13.0% in adult controls) and dorsal (50.0% P20 controls vs 29.0% in adult controls) sections when compared to the distribution of relay cells from adult control mice. The P20 control distribution also did not have any relay cells in the ventral sections of the NST, skewing the distribution towards the dorsal sections. Therefore, relay cells from the P20 and adult control populations are differently distributed along the dorsal-ventral axis of the NST. This is due in part to the large differences in the number of cells in each of these control groups. Finally, the dorsal-ventral distribution of P20 ENaC KO relay cells was not significantly different that of the adult control population ($X^2 (3) = 3.24$, $p=0.356$). Thus, despite the large differences in the number cells in these two ENaC KO populations, they are similarly sampled along the dorsal-ventral axis of the NST (Fig 3).

Relay Cells from Adult α ENaC Mice Have More Complex Dendritic Fields

There were no significant differences between the mean (\pm SEM) number of primary dendrites created by relay cells among P20 control (4.05 ± 0.31), adult control (3.72 ± 0.10), P20 α ENaC KO (3.65 ± 0.65), and adult α ENaC KO ($4.12 \pm$

0.16) mice (Fig 4A; $F(3,253) = 1.15$, $p = 0.330$). Likewise, the mean number of primary dendrites created by only the multipolar cells in each group was not significantly different (data not shown, $F(3,226) = 1.78$, $p = 0.151$). Therefore, the number of primary dendrites of NST relay cells did not change throughout development and was not dependent upon sodium taste activity.

While the number of primary dendrites was not affected by the removal of ENaC-mediated sodium taste activity, the number of dendritic branch points was affected. The mean (\pm SEM) number of branch points was 1.6x-1.8x greater in cells from adult α ENaC KO mice (7.30 ± 0.52) than it was in cells from P20 control (4.41 ± 0.55), adult control (4.09 ± 0.31), and P20 α ENaC KO mice (4.52 ± 0.81) -- this difference was significant (Fig 4B, $F(3,253) = 11.5$, $p < 0.0001$). The mean number of dendritic branch points created by relay cells from P20 control, adult control, and P20 α ENaC KO mice were not significantly different from each other (Fig 4B, $p < 0.05$).

Similar to the number of dendritic branch points, the total dendritic length created by relay cells from adult α ENaC KO mice was significantly greater than that of any other group (Fig 4C, $F(3,253) = 9.59$, $p < 0.0001$). The mean (\pm SEM) dendritic length (μm) in cells from adult α ENaC KO (692.76 ± 43.02) mice was 1.5-1.6x larger than that of cells from P20 control (441.51 ± 39.41), adult control (457.29 ± 24.69), and P20 α ENaC KO mice (448.95 ± 80.63). The mean dendritic length in relay cells from P20 control, adult control, and P20 α ENaC KO mice were not different from each other (Fig 4C, $p > 0.05$).

These large differences in the mean dendritic length and average dendritic branch points in the adult α ENaC KO relay cell population resulted in a similar difference in the mean dendritic complexity index (DCI)(Fig 4D). The DCI was calculated as follows: $DCI = (\text{sum of branch tip order} + \text{number of dendritic endings}) * (\text{total dendritic length} / \text{number of primary dendrites})$ (Pillai et al., 2012). Therefore, the DCI is a comprehensive measurement of the complexity a cell's dendritic field. The mean (\pm SEM) DCI in relay cells from adult α ENaC KO mice (7692.13 ± 1032.6) was 2.3-2.8x larger than that of relay cells from P20 control (2716.15 ± 475.01), adult control (3314.65 ± 502.57), and P20 α ENaC KO (2790.28 ± 501.15) mice (Fig 4D). These differences were statistically significant ($F(3,253) = 8.84, p < 0.0001$). Again, there were no significant differences among the mean DCI of relay cells from P20 control, adult control, and P20 α ENaC KO mice (Fig 4D, $p > 0.05$).

Relay Cells from Adult α ENaC Mice Have More Higher-Order Dendrites

The results above suggest that the increased complexity observed in relay cells from adult α ENaC KO mice are due to changes in the number and/or length of high order dendrites. To investigate this, we calculated the average frequency (Fig 5A), average dendritic length (Fig 5B), and average mean dendritic length (Fig 5C) of each order of dendrite for each group of cells. Statistical analysis found a significant effect of animal group on average frequency ($F(3,1771) = 35.7, p < 0.0001$), average dendritic length ($F(3,1771) = 16.3, p < 0.0001$), and average mean dendritic length ($F(3,1771) = 5.12, p = 0.002$).

Consistent with what was reported above, there were no differences in the mean number of primary dendrites among neurons from P20 control, adult control, P20 α ENaC KO, and adult α ENaC KO mice (Fig 5A, $p > 0.05$). There were also no differences in the average total dendritic lengths (Fig 5B) or average mean dendritic lengths (Fig 5C) of primary dendrites among neurons in P20 control, adult control, P20 α ENaC KO, or adult α ENaC KO mice ($p > 0.05$).

As was predicted, the Bonferroni post hoc test found that relay cells from adult α ENaC KO mice had significantly more second-order dendrites than cells from adult control mice ($p < 0.0001$). Specifically, cells from adult α ENaC KO mice had 1.3x more second-order dendrites than cells from adult control mice (Fig 5A). Similarly, there was also a significant difference in the average dendritic length associated with second-order dendrites between these two groups ($p = 0.004$). The dendritic length of second-order dendrites in cells from adult α ENaC KO mice was 1.2x larger than that of cells from adult control mice (Fig 5B). However, there was no difference in the mean dendritic length of second-order dendrites between cells from adult control and adult α ENaC KO mice (Fig 5C, $p = 0.986$). Taken together, these data suggest that cells from α ENaC KO mice are creating more second-order dendrites than cells from control mice, but the dendrites in α ENaC KO mice are not longer than they would be in control mice relay cells. None of the other groups were different from each in regards to the number of second-order dendrites created (Fig 5A, $p > 0.05$), the dendritic length associated with second-order dendrites (Fig 5B, $p > 0.05$), or the mean dendritic length of second-order dendrites (Fig 5C, $p > 0.05$).

The number and average dendritic length of third-order dendrites was also affected by removal of ENaC-mediated taste activity. Adult α ENaC KO mice relay cells in the NST averaged significantly more third-order dendrites than relay cells from adult control ($p < 0.0001$), P20 control ($p < 0.0001$), and P20 α ENaC KO ($p < 0.0001$) mice (Fig 5A). Similar to the trend found with second-order dendrites, the increased frequency of third-order dendrites in relay cells from adult α ENaC KO mice produced a significant increase in the average dendritic length associated with third order dendrites in these cells when compared to the adult control ($p < 0.0001$) or P20 ENaC KO ($p < 0.0001$) relay cell populations (Fig 5B). Again, suggesting third-order dendrites in cells from adult α ENaC KO mice were not extending further than they do in the other relay cell populations (Fig 5C, $p > 0.05$).

Fourth-order dendrites were also affected by removal of ENaC-mediated taste activity. The average mean number of fourth-order dendrites in the adult α ENaC KO mice relay cells was significantly larger than cells from adult control ($p < 0.0001$), P20 control ($p < 0.0001$), or P20 α ENaC KO ($p < 0.0001$) mice (Fig 5A). Specifically, cells from adult α ENaC KO mice averaged 2.5-3.0x more fourth-order dendrites than any other group of relay cells. The dendritic length associated with fourth-order dendrites showed a similar trend to the frequency of fourth-order dendrites. The dendritic length associated with fourth-order dendrites in relay cells from adult α ENaC KO mice was 2.2-4.7x greater than cells from adult control ($p = 0.0003$), P20 control ($p = 0.0024$), and P20 α ENaC KO ($p = 0.0007$) mice (Fig 5B). However, unlike third-order dendrites, the average mean dendritic length of fourth-order dendrites in adult α ENaC KO mice relay cells was significantly larger than that

of adult control mice relay cells (Fig 5C, $p = 0.0117$). This suggests that the increase in dendritic length cannot fully be explained by increases in the frequency of fourth-order dendrites (Fig 5A-C).

The frequency, dendritic length, and mean dendritic length associated with fifth-order dendrites were only significantly different between adult α ENaC KO mice relay cells and adult control mice NST cells. Specifically, relay cells from adult α ENaC KO mice averaged 3.0x more fifth-order dendrites than relay cells from adult control mice (Fig 5A; $p = 0.0085$). Similarly, the dendritic length associated with fifth-order dendrites in adult α ENaC KO mice was roughly 3.8x larger than that found in adult control mice (Fig 5B; $p = 0.0114$). The mean dendritic length of fifth-order dendrites was also significantly greater in relay cells than from adult α ENaC KO mice ($p = 0.0225$), suggesting that the increased dendritic length of fifth-order dendrites in cells from adult α ENaC KO mice was not only due to increases in the frequency of these dendrites within cells (Fig 5C).

Finally, there were no differences in the frequency, dendritic length, or mean dendritic length associated with sixth- or seventh-order dendrites among any groups of relay cells (Fig 5A-C; $p > 0.05$). This was due, in part, to very few cells having sixth- or seventh-order dendrites regardless of group.

In summary, removal of sodium taste activity throughout life resulted in the creation of more, high order dendrites in adulthood. Relay cells from adult α ENaC KO mice had more second- through fifth-order dendrites than did relay cells from P20 control, P20 α ENaC KO, or adult control mice (Fig 5A). These changes in the frequency of high order dendrites created by cells in adult α ENaC KO mice drove

similar changes the amount of dendritic material associated with higher-order dendrites in adult α ENaC KO mice relay cells when compared to other groups of relay cells (Fig 5B-C). However, the mean dendritic length associated with fourth- and fifth-order dendrites from adult α ENaC KO mice relay cells was larger than that of relay cells from adult control mice (Fig 5C), suggesting these dendrites also extended further than they did in adult control mice relay cells.

Gross Dendritic Morphology and Orientation of Relay Cells from Adult α ENaC KO Mice Appear Normal Despite Increased Dendritic Complexity

To assess how the increased dendritic complexity observed in relay cells from adult α ENaC KO mice affected the overall dendritic morphology, we did a Sholl analysis (see methods for details). Briefly, Sholl analyses use a series of concentric circles, centered upon the cell soma, to assess how dendritic architecture changes as the dendrites extend from the cell soma. Measurements such as the number of times dendrites intersect with each concentric circle (Fig 6A) and the amount of dendritic material within each ring (Fig 6B) are then collected to assess how the dendritic field is spatially organized.

Fig 6A shows the results from a Sholl analysis, calculating the mean number of times dendrites intersected with each concentric ring for each group of NST relay cells. As would be predicted from the dendritic complexity results discussed above, adult α ENaC KO mice relay cells averaged significantly more dendritic intersections than any other group of relay cells (Fig 6A; $F(3,11887) = 132, p < 0.0001$). However, these differences were only significant within the first 125 μ m from the cell soma, with slight differences in significance when comparing relay cells from adult α ENaC

KO mice to any other group. For example, comparing the number of intersections that adult α ENaC KO mice cells made to that of relay cells from adult control mice resulted in significant differences between 20-110 μ m from the cell soma (FIG 6A, $p < 0.05$). Comparing the number of intersections relay cells from adult α ENaC KO mice make to that of relay cells from P20 α ENaC KO mice resulted in significant differences between 35-95 μ m from the cell soma (FIG 6A, $p < 0.05$). Finally, there were also significant differences between the dendritic intersections of relay cells from adult α ENaC KO mice and relay cells from P20 control mice within 60-125 μ m from the cell soma (Fig 6A, $p < 0.05$). Thus, a majority of the changes in the dendritic architecture occurring in adult α ENaC KO mice relay cells happened within the first 125 μ m from the cell soma, relatively early in the dendritic field.

Further support of this idea can be seen in the results from a Sholl analysis assessing how dendritic length changed as a function of distance from the cell soma (Fig 6B). This analysis calculated the amount of dendritic material within each concentric ring rather than counting the number of times dendrites intersected with these concentric rings. Results from this analysis are similar to the results from the Sholl analysis discussed above. The amount of dendritic material created by relay cells from adult α ENaC KO mice was significantly higher than either P20 groups or the adult control group within the first 130 μ m of the cell soma (Fig 6B; $F(3,11887) = 161$, $p < 0.0001$). Again, there were slight differences in the areas of significance when comparing the adult α ENaC KO mice relay cells to any one of the other groups (Fig 6B, $p < 0.05$). However, unlike the data discussed above, we also found a significant difference between the relay cells from adult control mice and either P20

cell groups or the adult α ENaC KO cell group within 30 μ m from the cell body (Fig 6B; $p < 0.05$).

Interestingly, while relay cells from adult α ENaC KO mice had significantly more intersections and dendritic material than that in the adult control mice, the overall shape of the curves created in both Sholl analyses were similar. This finding suggests that the overall dendritic morphology of these two cell groups were similar, despite the differences in dendritic complexity and dendritic length. Likewise, comparing the shape of both curves from the two P20 groups with that of the adult control group implies that there is a subtle developmental reorganization of dendritic material. That is, there is a slight loss of dendritic material early in the dendritic field and an elaboration of dendritic fields further from the cell soma between P20 and adulthood. This idea is supported by the observation that relay cells from adult control mice created significantly less dendritic material than any other cell group within the first 30 μ m from the cell body (Fig 6B; $p < 0.05$).

We also asked if the removing ENaC-mediated taste activity altered the dendritic orientation preference that these NST relay cells usually maintain. Typically, these relay cells orient their dendritic fields parallel to the solitary tract, one of the major pathways for ascending gustatory information (Davis, 1988; Corson and Erisir, 2013). This results in a dendritic orientation preference that is roughly 30-45° off the horizontal (medial-lateral) axis. To assess if ENaC-mediated neural activity is necessary for these cells to create this orientation preference, we created polar histograms for each cell group (see methods for details). Figure 7 shows the resulting normalized polar histograms from each cell group. We found

that the P20 control and P20 α ENaC KO polar histograms were similar to each other, and relatively similar to that of the adult control relay cell group (Fig 7). There was a slight increase in the amount of dendritic material relay cells from adult control mice created in the medial caudal portion of their dendritic field compared to either P20 group. Regardless of these slight differences, both P20 groups and the adult control group had similar dendritic orientation preferences, roughly 45° off the horizontal (medial-lateral) axis, similar to what has been previously reported (Davis and Jang, 1988; Corson and Erisir, 2013). Interestingly, while the adult α ENaC KO relay cell polar histogram was larger than all other groups, reflecting their increased dendritic length reported above, the overall orientation preference of these cells was similar to that of the other three groups (Fig 7). Thus, the typical orientation preference that NST relay cells display develops rather early in an animal's life, before postnatal day 20, and does not require ENaC-mediated taste activity to occur.

Chorda Tympani Terminal Fields Develop Ectopically and do not “Prune” in Adult α ENaC KO Mice

We previously reported that ENaC-mediated taste activity is necessary for both the development and maintenance of gustatory terminal fields in the NST (Skyberg et al., 2017; Sun et al., 2017). Gustatory terminal field volumes in adult α ENaC KO mice, lacking ENaC-mediated taste activity throughout life, were approximately 2.4x larger than that of age-matched control mice. However, we do not know how the gustatory terminal fields in the NST organize in young, P20 mice, before ENaC-mediated taste experience matures and begins driving terminal field development. Therefore, to gain an understanding of the developmental trajectory

that these terminal fields take in both control and α ENaC KO mice, we labeled the chorda tympani (CT) nerve in P20 control and α ENaC KO mice. We chose to label only the CT, as it carries a majority of ENaC-mediated neural activity generated in the oral cavity. However, it should be noted that the GSP is also responsive to sodium taste stimulation and therefore also carries some sodium taste activity.

Fig 8 shows representative photomicrographs (Fig 8A-D) of the CT as well as quantification of the total CT terminal field volume (Fig 8E) for control and α ENaC KO mice at two developmental ages -- P20 and adulthood. Statistical analysis confirmed there was a significant difference in the total CT terminal field volume among groups ($F(3,18) = 42.7, p < 0.0001$). Comparing mean CT terminal field volumes between P20 control and adult control mice showed a clear developmental decrease in the overall size of the CT terminal field (Fig 8A-B, E). Between P20 and adulthood in control mice, the CT terminal field volume underwent a 1.7-fold decrease in volume, a difference that was statistically significant (Fig 8E, $p < 0.0001$). This developmental decrease in CT terminal field size was similar to what has been reported in rat (May and Hill, 2006; Mangold and Hill, 2008). As we reported previously (Sun et al., 2017), terminal fields in adult α ENaC KO mice were roughly 2.4x larger than that found in age-matched control mice. This difference was statistically significant (Fig 8E, $p < 0.0001$). Again, this difference indicates that ENaC-mediated taste activity was necessary for terminal fields to develop properly. The mean CT terminal field volumes in P20 control and P20 α ENaC KO mice were nearly identical ($p > 0.9999$), suggesting these terminal fields develop similarly before P20 and that ENaC-mediated neural activity only began driving terminal field

“pruning” after P20 (Fig 8A, C, E). Finally, we found an interesting difference between the CT terminal field volumes between P20 and adult α ENaC KO mice. Between P20 and adulthood, mean CT terminal field volumes underwent a 1.3-fold increase. This difference was also statistically significant (Fig 8C, D, E, $p = 0.0084$). Therefore, without ENaC-mediated taste activity terminal fields do not just fail to develop, they continue to grow.

Adult α ENaC KO Mice Have a Selective Loss of ENaC-Mediated Sodium Taste Activity Throughout Development

Figure 9 shows the integrated (Fig 9A-D) and normalized (Fig 9E-F) CT whole nerve responses to an increasing concentration series of NaCl in P20 control (Fig 9A, E), adult control (Fig 9B, E), P20 ENaC KO (Fig 9C, F), and adult ENaC KO (Fig 9D, F) mice. Comparing CT whole nerve responses from P20 control mice and adult control mice to an increasing concentration series of NaCl shows a clear developmental increase in ability of NaCl to drive CT responses (Fig 9A, B, E). This is particularly true when comparing CT responses to higher concentrations of NaCl. The relative responses to 0.25M and 0.5M NaCl in P20 control mice were significantly less (40-50%) than the respective responses in adult control mice (Fig 9E; $F(3,48) = 58.92$; significant posttest, $p = 0.0001 - 0.0001$). There were no significant differences between the relative responses to 0.05M and 0.1M NaCl in P20 control and adult control mice (Fig 9E; $p > 0.9999$). Interestingly, there was also a difference in NaCl responses after lingual application of amiloride between P20 control and adult control mice. Relative CT responses to 0.25M and 0.5M NaCl after amiloride from P20 mice were less (40-50%) than the respective responses in adult

control mice after amiloride. However, this difference was only significant when comparing the 0.5M NaCl responses after amiloride from P20 control and adult control mice (Fig 9E; $p = 0.006$). Therefore, it seems that there is a developmental increase in both the amiloride sensitive and amiloride insensitive salt transduction pathways in control mice between P20 and adulthood.

By comparison, conditionally deleting the *Scnn1a* gene from taste bud cells had selective effects on CT whole nerve taste responses. In adult α ENaC KO mice, increasing the concentration of NaCl did not result in increases in CT responses similar to what occurred in adult controls (Fig 9E). For example, the relative CT responses to 0.25M and 0.5M NaCl in adult α ENaC KO mice were significantly less (40-60%) than the respective responses in adult control mice (Fig 9E-F; $F(3,48) = 118.4$; significant posttests, $p = 0.0063 - 0.0001$). This is similar to what has been previously reported (Chandrashekar et al., 2010; Skyberg et al., 2017; Sun et al., 2017). Furthermore, the average CT responses to all concentrations of NaCl in P20 control mice and P20 ENaC KO mice were not significantly different from each other (Fig 9E-F; $p > 0.05$).

Importantly, the epithelial sodium channel blocker, amiloride, did not attenuate CT responses from either P20 or adult ENaC KO mice (Fig 9C, D, F), indicating two things. One, that removal of the *Scnn1a* gene was effective in eliminating ENaC-mediated taste activity, and two, the small remaining responses in these KO mice were mediated by an amiloride-insensitive transduction pathway. Interestingly, there was a slight developmental increase in the amiloride insensitive CT whole nerve responses between P20 and adulthood in our ENaC KO mice, similar

to what was seen in control mice (Fig 9E-F). These observations suggest that there may be a developmental change in the amiloride-insensitive salt transduction pathway in both control and ENaC KO mice. While the amiloride-insensitive pathway is not well understood, candidate gatekeepers for this transduction pathway include the vanilloid receptor-1 (VR-1) and/or inhibitory transepithelial potentials generated as cations in salt stimuli permeate through tight junctions, leaving behind their larger anions (Lyll et al., 2004; Lewandowski et al., 2016). This anion build up is then thought to act as an inhibitory local field potential, preventing depolarization of the cell and the proper movement of cations (Lewandowski et al., 2016). While the exact mechanism(s) by which the amiloride-insensitive pathway generates taste-elicited responses is still not fully categorized, the observation that it may also undergo a developmental increase in function between P20 and adulthood is novel and raises interesting questions regarding the molecular/cellular changes underlying this development.

In summary, between P20 and adulthood there is an ENaC-mediated developmental increase in the ability of NaCl to drive whole nerve responses in control mice (Fig 9E). Removal of the *Scnn1a* gene in our ENaC KO mice prevents this developmental increase in the amiloride-sensitive CT responses and prevented sodium-elicited taste activity from entering the central gustatory system (Fig 9F). Finally, we found that there may also be a similar developmental change in the amiloride-insensitive pathway in both control and ENaC KO mice (Fig 9E-F).

Discussion

Deletion of the gene responsible for α ENaC in mouse taste buds beginning embryonically and continuing throughout life had significant effects on the development and organization of gustatory circuits in the NST. Both the presynaptic CT terminal field size and the dendritic complexity of the postsynaptic NST relay cells were 2-3x larger in adult α ENaC KO mice than in adult age-matched control mice. Thus, we show that ENaC-mediated neural activity is necessary for the gustatory NST circuit to develop properly. Furthermore, we also show that these substantial changes in terminal field size and dendritic field complexity occur after P20, an age when ENaC-mediated neural activity is just beginning to mature in normally-developing mice. Collectively, these data suggest that there is a period of considerable reorganization in the central gustatory circuitry after P20 in both control mice with normal taste experience and in ENaC KO mice lacking sodium taste experience.

Development of Gustatory NST Circuitry in Control Mice

We show here that the dendritic organization of NST relay cells in control mice do not undergo significant developmental changes between P20 and adulthood. The number of primary dendrites (Fig 4A), number of dendritic branch points (Fig 4B), total dendritic length (Fig 4C), and overall dendritic complexity (Fig 4D) of NST relay cells from P20 and adult control mice were not different from each other, illustrating that a majority of the development of these dendritic fields is complete by P20. There were also no significant differences in the number of dendrites (Fig 5A) or dendritic lengths (Fig 5B) associated with first- through seventh-order dendrites between P20 and adult control relay cells, which provides

further evidence supporting the idea that dendritic fields of these cells are mature by P20. However, the dendritic morphologies of these two populations of control NST relay cells were not identical. Sholl analyses of these two cellular populations resulted in slightly different shaped curves (Fig 6). The curve created by P20 control relay cells has a higher peak within the first 50 μ m from the cell soma and plateaus earlier than the curve created by the adult control relay cells (Fig 6). Put another way, relay cells from P20 control mice have more dendritic material within the first 50 μ m from the cell soma and have less dendritic material further from the cell soma than do relay cells from adult control mice (Fig 6). This suggests that there is a slight loss of dendritic material close to the cell soma and an elaboration of dendritic material further from the cell soma between P20 and adulthood. Regardless, by P20 a majority of the development of NST relay cell dendritic fields is complete. This timeline is similar, although not identical, to the developmental trends observed in the dendrites of NST cells in the sheep (Mistretta and Labyak, 1994) and rat (Lasiter et al., 1989; Bao et al., 1995). In rat, the dendritic architecture of NST cells increases in complexity between birth and postnatal day 20-30 (Lasiter et al., 1989; Bao et al., 1995). Accompanying this development are changes in both the intrinsic electrophysiological properties of these cells as well as taste-elicited extracellular responses (Hill et al., 1983; Bao et al., 1995). This suggests that physiological and functional changes accompany the changes in dendritic architecture discussed above. Future research will be necessary to fully delineate this relationship.

Unlike the dendritic fields of relay cells in the NST, the presynaptic terminal fields of gustatory afferents from the oral cavity undergo extensive changes in size

after P20. Between P15 and P30 the CT terminal field reorganizes, resulting in a 2-fold decrease in terminal field volume (Fig 8; Zheng et al., 2014). Around P30 these terminal fields reach a mature organization and are maintained in this state throughout the rest of an animal's life (Zheng et al., 2014). Thus, there are some interesting differences in the developmental timelines of the presynaptic terminal fields of gustatory afferents and the postsynaptic dendritic fields of relay cells in the NST. The dendritic fields of relay cells in the NST are mature by P20, well before the terminal fields of gustatory afferents have matured. Thus, a causal relationship between the development of these pre- and postsynaptic cells in the NST is not readily apparent. Further insights into the relationship between the development of the pre- and postsynaptic cells in this circuit may be accomplished by investigating how synapses in this circuit change with age. In fact, Wang et al. (2012) found an age-dependent decrease in the number of synapses that CT terminals have in the rat NST, as would be predicted by the developmental decreases in total CT terminal field volume in rat (May and Hill, 2006; Mangold and Hill, 2008) and mouse (Fig 8; Zheng et al., 2014). They also report a substantial developmental decrease in the number of synapses of CT terminals onto GABAergic targets (Wang et al., 2012). Consequently, CT terminal field "pruning" may reflect a loss of synapses between CT terminals and non-relay cell targets in the NST, potentially explaining why the NST relay cell dendritic fields appear mature before the CT terminal fields. Alternatively, Hill et al. (1983) report a developmental increase in the number of impulses per second created by rat NST relay neurons to certain taste stimuli (Hill et al., 1983). This increase in response frequency cannot be explained by increases in the

response frequencies created by the same taste stimuli in CT afferent fibers, suggesting there is a developmental reorganization of CT synapses onto postsynaptic NST relay cells. That is, there is convergence of gustatory information from CT afferent fibers to NST relay cells driven primarily by changes at the synaptic level within this circuit. Thus, changes in the number, location, and/or efficacy of synapses in this circuit may be essential in explaining the differences seen in the anatomical development of pre- and postsynaptic cells in the gustatory NST circuit.

Development of Gustatory NST Circuitry in α ENaC KO Mice

Removal of ENaC-mediated taste activity had large effects on the organization and development of both the presynaptic gustatory terminal fields and the postsynaptic dendritic fields. The mean total terminal field volume and mean dendritic complexity of NST relay cells in adult α ENaC KO mice were 2.3-2.4x larger than that found in age-matched control mice. Importantly, adult α ENaC KO mice have a selective, diminished CT whole nerve responses to a concentration series of NaCl when compared to age-matched controls (Fig 9; Chandrashekar et al., 2010; Sun et al., 2017). Thus, neural activity is a necessary regulator of the development and/or maintenance of gustatory circuitry in the NST. Removal of ENaC-mediated sodium taste activity, beginning embryonically and continuing throughout development prevents the normal "pruning" of CT terminals (Fig 8) and also results in ectopic expansion of dendritic fields (Fig 4D) of NST relay cells and CT terminal fields (Fig 8). Remarkably, these differences were not present in immature, P20 mice -- the mean CT terminal field volume (Fig 8) and mean dendritic complexity (Fig 4D) of NST relay cells were not different between P20 control and P20 α ENaC

KO mice. This fits with the hypothesis that neural activity, or lack thereof, is responsible for the differences discussed above, as ENaC-mediated neural activity is just beginning to mature at P20 in normally-developing mice (Fig 9). Therefore, there is an important developmental period after P20 in which gustatory circuitry in the NST normally organizes in control mice with normal taste experience and ectopically reorganizes in α ENaC KO mice lacking sodium taste experience.

Role of ENaC-Mediated Activity in Development and Maintenance of Gustatory NST Circuitry

The results from these and other experiments illustrate multiple effects of removing ENaC-mediated sodium taste activity throughout an animal's life. Indeed, the effects of removing ENaC activity on the terminal and dendritic fields were not identical. In the case of the terminal fields of gustatory afferents, the normal developmental decrease in terminal field size was prevented in ENaC KO mice, suggesting that sodium salt activity can drive this developmental "pruning" of terminal fields in the NST (Sun et al., 2017). We have also shown that the maintenance of these terminal fields at a mature state is dependent upon ENaC-mediated sodium taste activity, without which terminal fields revert back to an immature, enlarged organization (Skyberg et al., 2017). The dendritic fields show a different dependence upon this ENaC activity. Because the dendritic fields resemble a mature organization by P20 in control mice, which is before ENaC-mediated activity has fully matured, it is unlikely that this post weaning reorganization is driven by ENaC activity. However, similar to terminal fields, the maintenance of NST dendritic fields after P20 are dependent upon ENaC-mediated sodium taste activity

(Fig 4). Therefore, while there are differences in the specific ways ENaC activity modulates the pre- and postsynaptic elements of the gustatory NST circuit, removing this ENaC-mediated activity always results in an elaboration of the elements within this circuit (Skyberg et al., 2017; Sun et al., 2017). One intriguing explanation for this observation is that dendritic and axonal elongation are the default growth patterns for these gustatory cells and neuronal activity competes against this innate program. In fact, this has been proposed to occur during the morphological development of retinogeniculate axons in the dLGN (Stretavan et al., 1988) as well as during dendritic development of Purkinje cells in the murine cerebellum (Schilling et al., 1991).

Remaining Questions

One unique benefit of using α ENaC KO mice as a model to assess the roles neural activity plays in the development and organization of gustatory circuitry is that these mice only lack activity from a single transduction pathway and a single taste modality (salty) (Chandrashekar et al., 2010; Skyberg et al., 2017; Sun et al., 2017). The specificity of our knockout model gives rise to a few interesting questions regarding the results of the experiments discussed above. First, if we are only removing neural activity from one specific taste modality, are we also only altering the dendritic architecture of a certain subset of taste responsive NST relay cells? In an attempt to answer this, we plotted the percentage of cells from adult control and adult α ENaC KO mice as a function of their highest dendritic order (Fig 10). The resultant curves from adult control and α ENaC KO mice were nearly identical with one exception -- the α ENaC KO curve was shifted to the right by one

dendritic order. This shift suggests there may not be one subpopulation of cells within the NST that are increasing in complexity due to our manipulation between these two adult cell populations. Instead it seems that there is an increase in the dendritic complexity for the entire population in cells in adult α ENaC KO mice compared to cells from adult control mice. In support of this idea is the observation that a large majority of taste responsive cells in the adult rodent NST are broadly tuned and respond to more than one taste stimuli (Hill et al., 1983; Sato and Beidler, 1997; Cho et al., 2002; Carleton et al., 2010). Therefore, removal of sodium taste activity in our α ENaC KO mice is likely affecting many taste responsive relay cells in the NST rather than one specific subpopulation. Interestingly, individual CT fibers are not nearly as broadly tuned as NST relay cells (Ogawa et al., 1968; Frank, 1973; Pfaffmann, 1974; Pfaffmann et al., 1976), indicating there is convergence of differential taste information onto NST relay cells. Therefore, it seems likely that removal of sodium taste activity in our α ENaC KO mice is affecting a majority of cells in the NST, rather than a certain subpopulation of taste responsive relay cells.

Another interesting question raised by the use of this specific knockout model is whether the effects discussed above are specific to sodium taste activity? We chose to alter sodium taste activity because it exhibits a twofold increase in response magnitude throughout development, as assessed by CT whole nerve recordings (Fig 9; S. L. Corson & Hill, 2011; David L. Hill & Bour, 1985; Mangold & Hill, 2008; Vogt & Hill, 1993). However, in mouse, sucrose taste activity also undergoes a similar, albeit lesser, increase in response magnitude (unpublished data). Therefore, sucrose taste activity may play a similar role in the development

and/or maintenance of central gustatory circuitry. Alternatively, the effects discussed above may not be specific to any one type of neural activity and instead be a result of changes in the overall amount of neural activity entering the central gustatory system.

One final consideration arising from the data presented above is how long a period of diminished taste experience is necessary to produce the ectopic growth in terminal fields and dendritic architecture. In these experiments, sodium taste experience was genetically removed throughout life, beginning embryonically. However, ENaC activity does not begin until around P20 in normally developing mice and thus the effects of the genetic manipulation (i.e. reduced sodium taste experience) in our ENaC KO mice are not manifested until around this age as well. Therefore, our adult ENaC KO mice are experiencing about 60 days of diminished sodium taste experience before their relay cells are retrogradely filled. This is a long period for these changes to occur and may not be necessary to produce the dendritic effects. Future research focusing on the time needed to create these wholesale changes in the development of pre- and postsynaptic elements of the gustatory NST circuit by retrogradely filling relay cells at different ages (e.g., P30) may help us fully understand the unique levels of plasticity observed in this system throughout life.

Citations

- Armstrong RA (2014) When to use the Bonferroni correction. *Ophthalmic Physiol Opt* 34:502–508.
- Bao H, Bradley RM, Mistretta CM (1995) Development of intrinsic electrophysiological properties in neurons from the gustatory region of rat nucleus of solitary tract. *Dev brain Res* 86:143–154.
- Brunjes P (1994) Unilateral naris closure and olfactory system development. *Brain Res Rev* 19:146–160.
- Butts DA, Kanold PO, Shatz CJ (2007) A burst-based “Hebbian” learning rule at retinogeniculate synapses links retinal waves to activity-dependent refinement. *PLoS Biol* 5:0651–0661.
- Cang J, Rentería RC, Kaneko M, Liu X, Copenhagen DR, Stryker MP (2005) Development of precise maps in visual cortex requires patterned spontaneous activity in the retina. *Neuron* 48:797–809.
- Carleton A, Accolla R, Simon S (2010) Coding in the mammalian gustatory system. *Trends Neurosci* 33:326–334.
- Chandrashekar J, Kuhn C, Oka Y, Yarmolinsky DA, Hummler E, Ryba NJP, Zuker CS (2010) The cells and peripheral representation of sodium taste in mice. *Nature* 464:297–301.
- Cho YK, Li C-S, Smith D V (2002) Taste responses of neurons in the hamster solitary nucleus are modulated by the central nucleus of the amygdala. *J Neurophysiol* 88:2979–2992.
- Corson JA, Erisir A (2013) Monosynaptic convergence of chorda tympani and

glossopharyngeal afferents onto ascending relay neurons in the nucleus of the solitary tract: A high-resolution confocal and correlative electron microscopy approach. *J Comp Neurol* 521:2907–2926.

Corson SL, Hill DL (2011) Chorda Tympani Nerve Terminal Field Maturation and Maintenance Is Severely Altered Following Changes to Gustatory Nerve Input to the Nucleus of the Solitary Tract. *J Neurosci* 31:7591–7603.

Davis BJ (1988) Computer-generated rotation analyses reveal a key three-dimensional feature of the nucleus of the solitary tract. *Brain Res Bull* 20:545–548.

Davis BJ, Jang T (1988) A Golgi analysis of the gustatory zone of the nucleus of the solitary tract in the adult hamster. *J Comp Neurol* 278:388–396.

El-Danaf RN, Krahe TE, Dilger EK, Bickford ME, Fox MA, Guido W (2015) Developmental remodeling of relay cells in the dorsal lateral geniculate nucleus in the absence of retinal input. *Neural Dev* 10:1–17.

Erickson RP (1966) Nontraumatic headholders for mammals. *Physiol Behav* 1:97–98.

Fekete Z, Pálfi E, Márton G, Handbauer M, Bérces Z, Ulbert I, Pongrácz A, Négyessy L (2015) In vivo iontophoretic BDA injection through a buried microfluidic channel of a neural multielectrode. *Procedia Eng* 120:464–467.

Frank ME (1973) An analysis of hamster afferent taste nerve response functions. *J Gen Physiol* 61:588–618.

Friedlander MJ, Stanford LR, Sherman SM (1982) Effects of monocular deprivation on the structure-function relationship of individual neurons in the cat's lateral

- geniculate nucleus. *J Neurosci* 2:321–330.
- Ganchrow D, Ganchrow JR, Cicchini V, Bartel DL, Kaufman D, Girard D, Whitehead MC (2014) Nucleus of the solitary tract in the C57BL/6J mouse: Subnuclear parcellation, chorda tympani nerve projections, and brainstem connections. *J Comp Neurol* 522:1565–1596.
- Guido W (2008) Refinement of the retinogeniculate pathway. *J Physiol* 586:4357–4362.
- Guillery RW (1973) Quantitative studies of transneuronal atrophy in the dorsal lateral geniculate nucleus of cats and kittens. *J Comp Neurol* 149:423–437.
- Hellekant G, af Segerstad CH, Roberts T, van der Wel H, Brouwer JN, Glaser D, Haynes R, Eichberg JW (1985) Effects of gymnemic acid on the chorda tympani proper nerve responses to sweet, sour, salty and bitter taste stimuli in the chimpanzee. *Acta Physiol Scand* 124:399–408.
- Hill DL, Bour TC (1985) Addition of functional amiloride-sensitive components to the receptor membrane: A possible mechanism for altered taste responses during development. *Dev Brain Res* 20:310–313.
- Hill DL, Bradley RM, Mistretta CM (1983) Development of taste responses in rat nucleus of solitary tract. *J Neurophysiol* 50:879–895.
- Hooks BM, Chen C (2006) Distinct Roles for Spontaneous and Visual Activity in Remodeling of the Retinogeniculate Synapse. *Neuron* 52:281–291.
- Hooks BM, Chen C (2008) Vision Triggers an Experience-Dependent Sensitive Period at the Retinogeniculate Synapse. *J Neurosci* 28:4807–4817.
- Jaubert-Miazza L, Green E, Lo FS, Bui K, Mills J, Guido W (2005) Structural and

functional composition of the developing retinogeniculate pathway in the mouse. *Vis Neurosci* 22:661–676.

Kaneko T, Saeki K, Lee T, Mizuno N (1996) Improved retrograde axonal transport and subsequent visualization of tetramethylrhodamine (TMR) -dextran amine by means of an acidic injection vehicle and antibodies against TMR. *J Neurosci Methods* 65:157–165.

Katz L, Shatz CJ (1996) Synaptic Activity and the Construction of Cortical Circuits. *Science* (80-) 274:1133–1138.

King C, Hill DL (1991) Dietary sodium chloride deprivation throughout development selectively influences the terminal field organization of gustatory afferent fibers projecting to the rat nucleus of the solitary tract. *J Comp Neurol* 303:159–169.

Krimm RF, Hill DL (1997) Early prenatal critical period for chorda tympani nerve terminal field development. *J Comp Neurol* 378:254–264.

Lasiter PS, Wong DM, Kachele DL (1989) Postnatal development of the rostral solitary nucleus in rat: Dendritic morphology and mitochondrial enzyme activity. *Brain Res Bull* 22:313–321.

Leake P, Hradek G, Chair L, Snyder R (2006) Neonatal deafness results in degraded topographic specificity of auditory nerve projections to the cochlear nucleus in cats. *J Comp Neurol* 497:13–31.

Lee L-J, Lo F-S, Erzurumlu R (2005) NMDA Receptor-Dependent Regulation of Axonal and Dendritic Branching. *J Neurosci* 25:2304–2311.

Lewandowski BC, Sukumaran SK, Margolskee RF, Bachmanov AA (2016) Amiloride-Insensitive Salt Taste Is Mediated by Two Populations of Type III Taste Cells

- with Distinct Transduction Mechanisms. *J Neurosci* 36:1942–1953.
- Lyall V, Heck GL, Vinnikova AK, Ghosh S, Phan THT, Alam RI, Russell OF, Malik SA, Bigbee JW, DeSimone JA (2004) The mammalian amiloride-insensitive non-specific salt taste receptor is a vanilloid receptor-1 variant. *J Physiol* 558:147–159.
- Mangold JE, Hill DL (2008) Postnatal reorganization of primary afferent terminal fields in the rat gustatory brainstem is determined by prenatal dietary history. *J Comp Neurol* 509:594–607.
- Matthews MR, Cowan WM, Powell TPS (1960) Transneuronal cell degeneration in the lateral geniculate nucleus of the macaque monkey. *J Anat* 94:145–169.
- May O, Hill DL (2006) Gustatory terminal field organization and developmental plasticity in the nucleus of the solitary tract revealed through triple fluorescence labeling. *J Comp Neurol* 497:658–669.
- Mistretta CM, Labyak SE (1994) Maturation of neuron types in nucleus of solitary tract associated with functional convergence during development of taste circuits. *J Comp Neurol* 345:359–376.
- Ogawa BYH, Sato M, Yamashita S (1968) Multiple sensitivity of chorda tympani fibres of the rat and hamster to gustatory and thermal stimuli. *J Physiol London*:223–240.
- Pfaffmann C (1974) Specificity of the sweet receptor in the squirrel monkey. *Chem Senses* 1:61–67.
- Pfaffmann C, Frank ME, Bartoshuk LM, Snell TC (1976) Coding of gustatory information in the squirrel monkey chorda tympani. *Prog Psychobiol Physiol*

Psychol 6:1–27.

Pillai AG, de Jong D, Kanatsou S, Krugers H, Knapman A, Heinzmann JM, Holsboer F, Landgraf R, Joëls M, Touma C (2012) Dendritic morphology of Hippocampal and Amygdalar neurons in adolescent mice is resilient to genetic differences in stress reactivity. *PLoS One* 7.

Reiner A, Veenman CL, Medina L, Jiao Y, Del Mar N, Honig MG (2000) Pathway tracing using biotinylated dextran amines. *J Neurosci Methods* 103:23–37.

Sato T, Beidler LM (1997) Broad tuning of rat taste cells for four basic taste stimuli. *Chem Senses* 22:287–293.

Schilling K, Dickinson MH, Connor JA, Morgan JI (1991) Electrical Activity in Cerebellar Cultures Determines Purkinje Cell Dendritic Growth Patterns. *Neuron* 7:1–12.

Shingai T, Beidler LM (1985) Response characteristics of three taste nerves in mice. *Brain Res* 335:245–249.

Sholl D (1956) Dendritic organization in the neurons of the visual and motor cortices of the cat. *J Anat* 87:387–406.1.

Skyberg R, Sun C, Hill DL (2017) Maintenance of Mouse Gustatory Terminal Field Organization is Disrupted Following Selective Removal of Peripheral Sodium Salt Taste Activity at Adulthood. *J Neurosci* 37:7619–7630.

Sollars SI, Walker BR, Thaw a. K, Hill DL (2006) Age-related decrease of the chorda tympani nerve terminal field in the nucleus of the solitary tract is prevented by dietary sodium restriction during development. *J Neurosci* 137:1229–1236.

Spector AC, Glendinning JI (2009) Linking peripheral taste processes to behavior.

- Curr Opin Neurobiol 19:370–377.
- Spector AC, Travers SP (2005) The representation of taste quality in the mammalian nervous system. *Behav Cogn Neurosci Rev* 4:143–191.
- Stellwagen D, Shatz CJ (2002) An instructive role for retinal waves in the development of retinogeniculate connectivity. *Neuron* 33:357–367.
- Sun C, Dayal A, Hill DL (2015) Expanded terminal fields of gustatory nerves accompany embryonic BDNF overexpression in mouse oral epithelia. *J Neurosci* 35:409–421.
- Sun C, Hummler E, Hill DL (2017) Selective Deletion of Sodium Salt Taste during Development Leads to Expanded Terminal Fields of Gustatory Nerves in the Adult Mouse Nucleus of the Solitary Tract. *J Neurosci* 37:660–672.
- Thompson A, Gribizis A, Chen C, Crair MC (2017) Activity-dependent development of visual receptive fields. *Curr Opin Neurobiol* 42:136–143.
- Tokita K, Boughter JD (2016) Topographic organizations of taste-responsive neurons in the parabrachial nucleus of C57BL/6J mice: An electrophysiological mapping study. *J Neurosci* 316:151–166.
- Tokita K, Inoue T, Boughter JD (2009) Afferent connections of the parabrachial nucleus in C57BL/6J mice. *J Neurosci* 161:475–488.
- Vogt MB, Hill DL (1993) Enduring alterations in neurophysiological taste responses after early dietary sodium deprivation. *J Neurophysiol* 69:832–841.
- Wang S, Corson J, Hill D, Erisir A (2012) Postnatal development of chorda tympani axons in the rat nucleus of the solitary tract. *J Comp Neurol* 520:3217–3235.
- Whitehead MC (1988) Neuronal architecture of the nucleus of the solitary tract in

the hamster. *J Comp Neurol* 276:547–572.

Whitehead MC (1990) Subdivisions and Neuron Types of the Nucleus of the Solitary Tract That Project to the Parabrachial Nucleus in the Hamster. *J Comp Neurol* 574:554–574.

Wiesel TN, Hubel DH (1963) Effects of visual deprivation on morphology and physiology of cells in the cat's lateral geniculate body. *J Neurophysiol* 26:978–993.

Zheng S, Sun C, Hill DL (2014) Postnatal reorganization of primary gustatory afferent terminal fields in the mouse brainstem is altered by prenatal dietary sodium history. In: Society for Neurosciences.

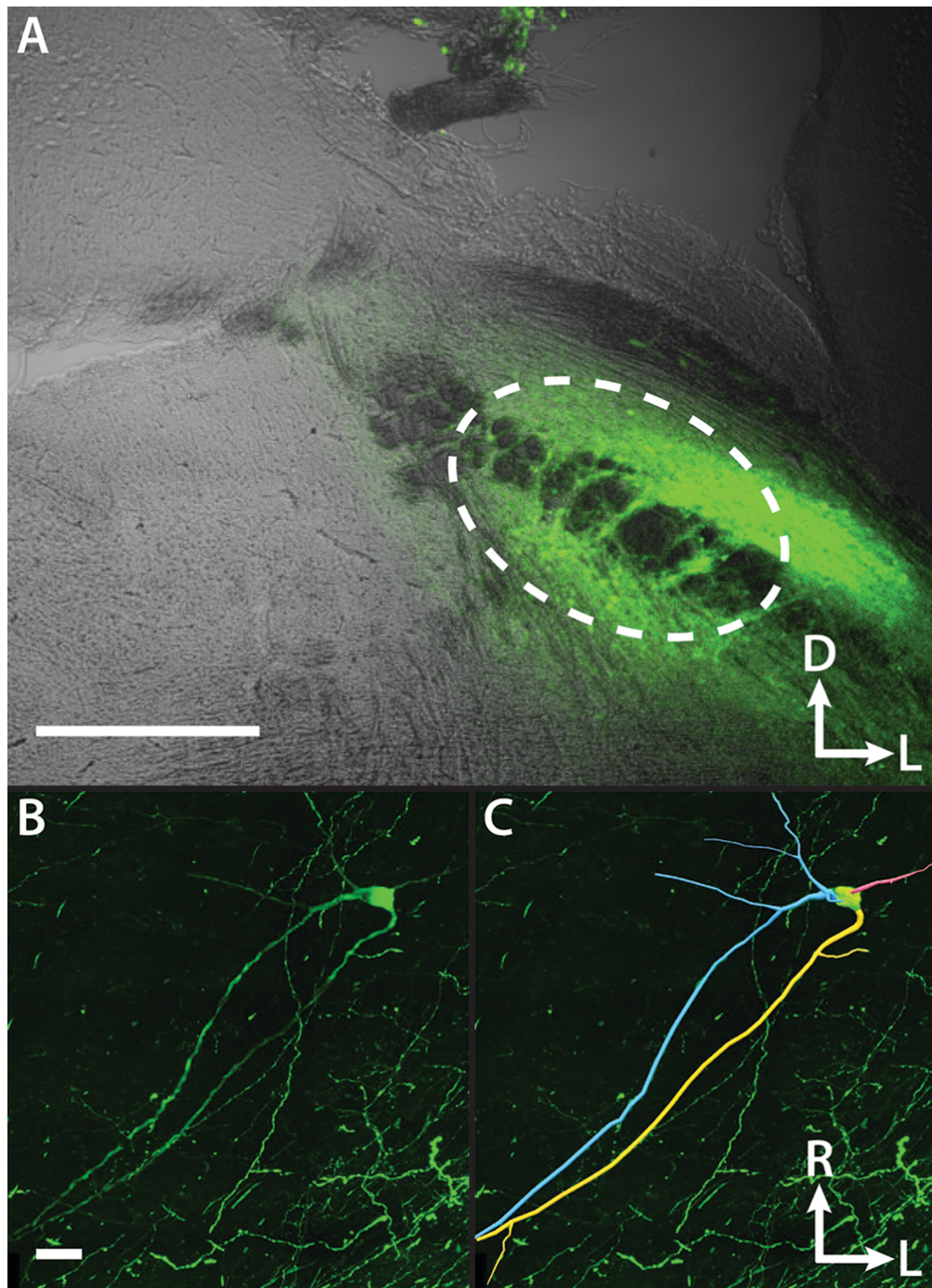


Figure 1. Stereotaxic injections into the waist region of the PBN result in robust retrograde labeling of relay cells in the NST. **A**, Coronal section through the PBN showing a stereotaxically-guided injection of 10% BDA (green) into the waist region of the right PBN (outlined in white dotted line). Photomicrograph taken at 4x. Scale bar in A, 500 μ m. D, dorsal; L, lateral. **B**, Horizontal section through the right NST showing a retrogradely-labeled NST relay cell following an injection of 10% BDA into the right PBN. Photomicrograph taken at 60x. **C**, Tracing of the same NST relay cell shown in B. Scale bar in B, 20 μ m and also applies to C. R, rostral; L, lateral.

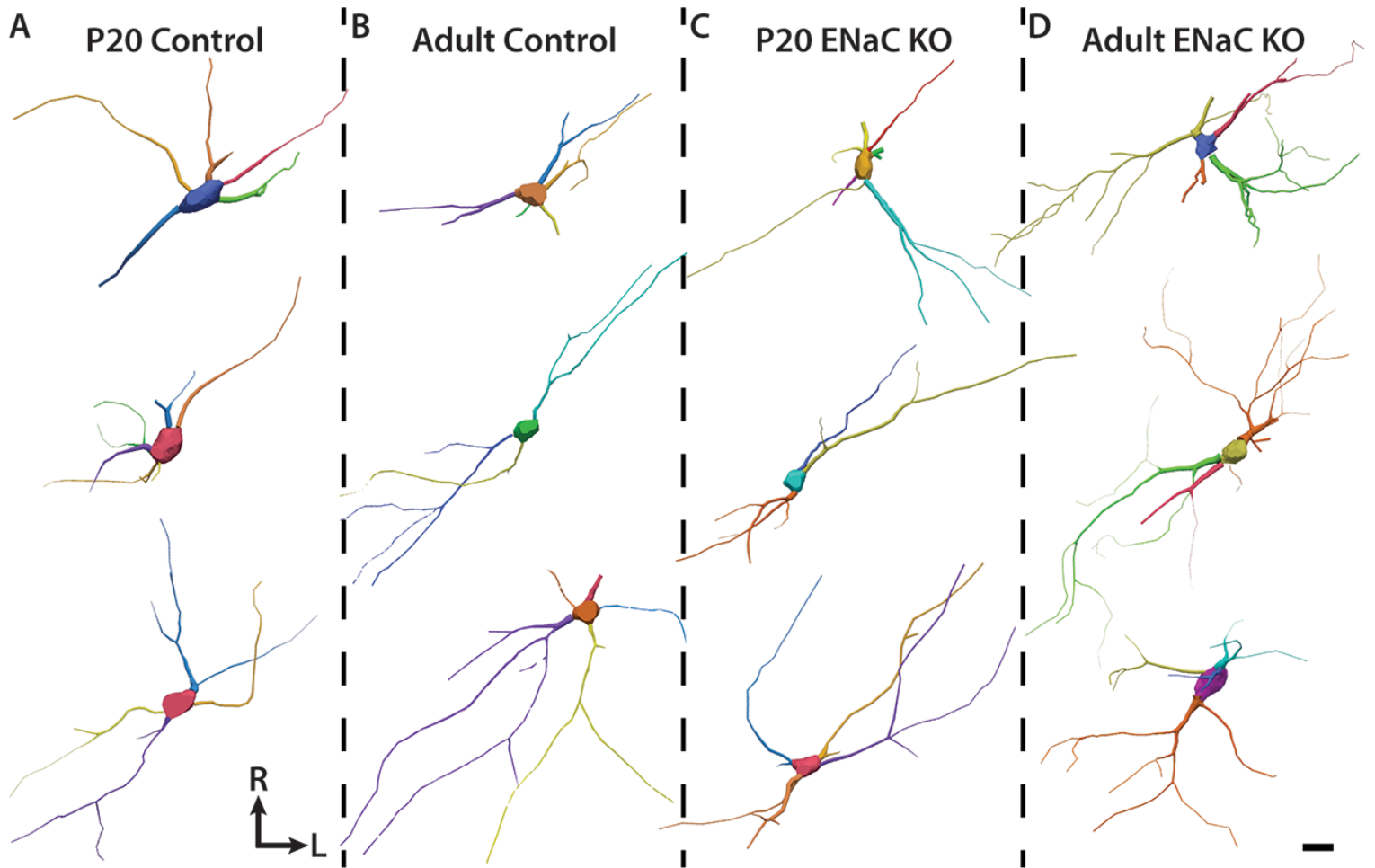


Figure 2. Representative NST relay cell tracings from P20 control mice (A), adult control mice (B), P20 ENaC KO mice (C), and adult ENaC KO mice (D). Scale bar in D, 20 μ m and applies to all panels. R, rostral; L, lateral.

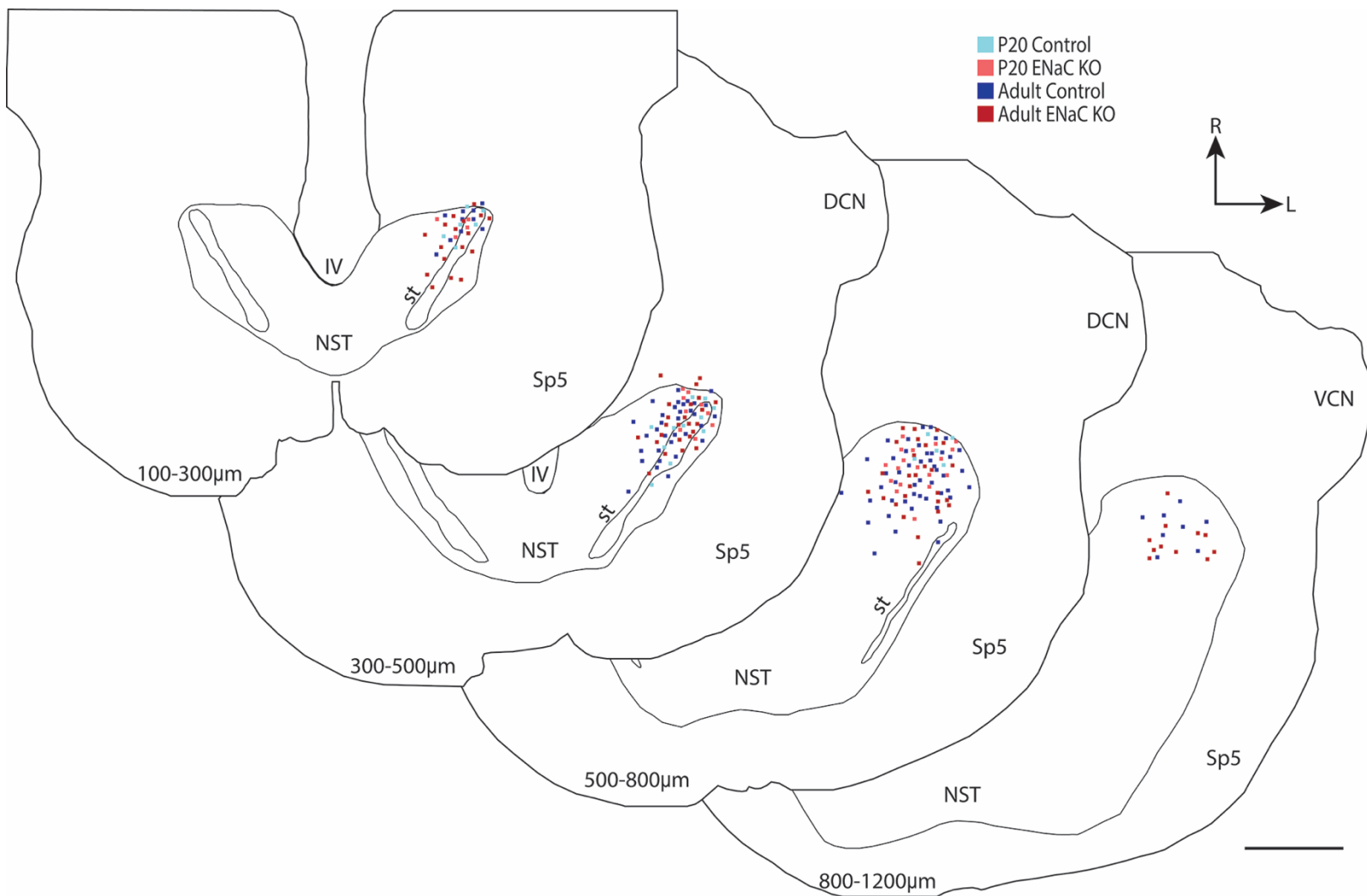


Figure 3. Relay cell locations throughout the dorsal ventral axis of the NST. The location of each P20 control (light blue), adult control (dark blue), P20 ENaC KO (light red), and adult ENaC KO (dark red) cell is projected onto representative tracings of the horizontally-sectioned brainstem throughout the dorsal ventral axis. Numbers on the bottom of each tracing illustrate the approximate distance from the top of the brainstem for each section is located. Scale bar, 500µm. IV, fourth ventricle; NST, nucleus of the solitary tract; st, solitary tract; Sp5, spinal trigeminal nucleus; DCN, dorsal cochlear nucleus; VCN, ventral cochlear nucleus; R, rostral; L, lateral.

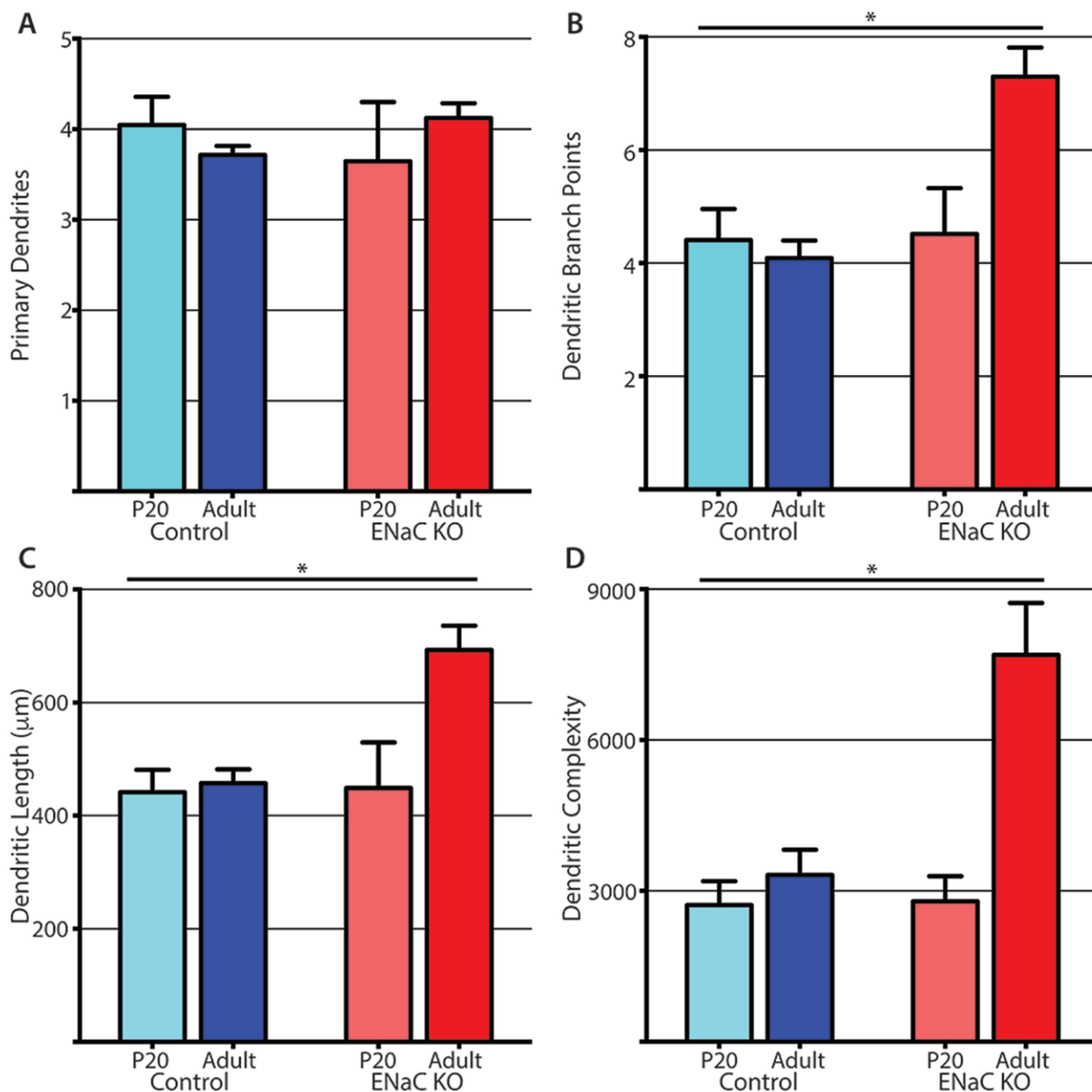


Figure 4. Dendritic characteristics of NST relay cells. **A**, Mean (\pm SEM) number of primary dendrites in relay cells from P20 control (light blue), adult control (dark blue), P20 ENaC KO (light red), and adult ENaC KO (dark red) mice. **B**, Mean (\pm SEM) number of dendritic branch points in relay cells from P20 control (light blue), adult control (dark blue), P20 ENaC KO (light red), and adult ENaC KO (dark red) mice. **C**, Mean (\pm SEM) total dendritic length (μm) from relay cells from P20 control (light blue), adult control (dark blue), P20 ENaC KO (light red), and adult ENaC KO (dark red) mice. **D**, Mean (\pm SEM) dendritic complexity (see methods for details) of relay cells from P20 control (light blue), adult control (dark blue), P20 ENaC KO (light red), and adult ENaC KO (dark red) mice. * $< p$ 0.05

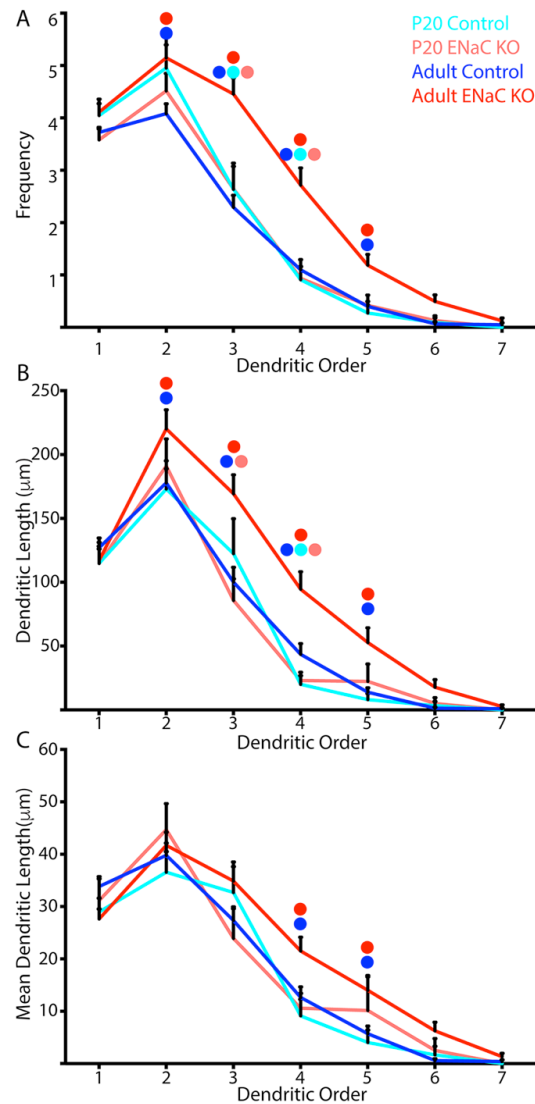


Figure 5. Dendritic characteristics by dendritic order. **A**, Average (\pm SEM) number of dendrites by dendritic order in relay cells from P20 control (light blue), adult control (dark blue), P20 ENaC KO (light red), and adult ENaC KO (dark red) mice. **B**, Average (\pm SEM) total dendritic length of dendrite by dendritic order in relay cells from P20 control (light blue), adult control (dark blue), P20 ENaC KO (light red), and adult ENaC KO (dark red) mice. **C**, Average (\pm SEM) mean dendritic length of dendrite by dendritic order in relay cells from P20 control (light blue), adult control (dark blue), P20 ENaC KO (light red), and adult ENaC KO (dark red) mice. Colored circles above each data point denote groups that are significantly different from each other ($p < 0.05$). For example, in A, the frequency of second-order dendrites in relay cells from adult ENaC KO mice (dark red) is only significantly different from that of adult control mice (dark blue). Conversely, the frequency of third-order dendrites in relay cells from adult ENaC KO mice (dark red) is significantly greater than that of any other other group.

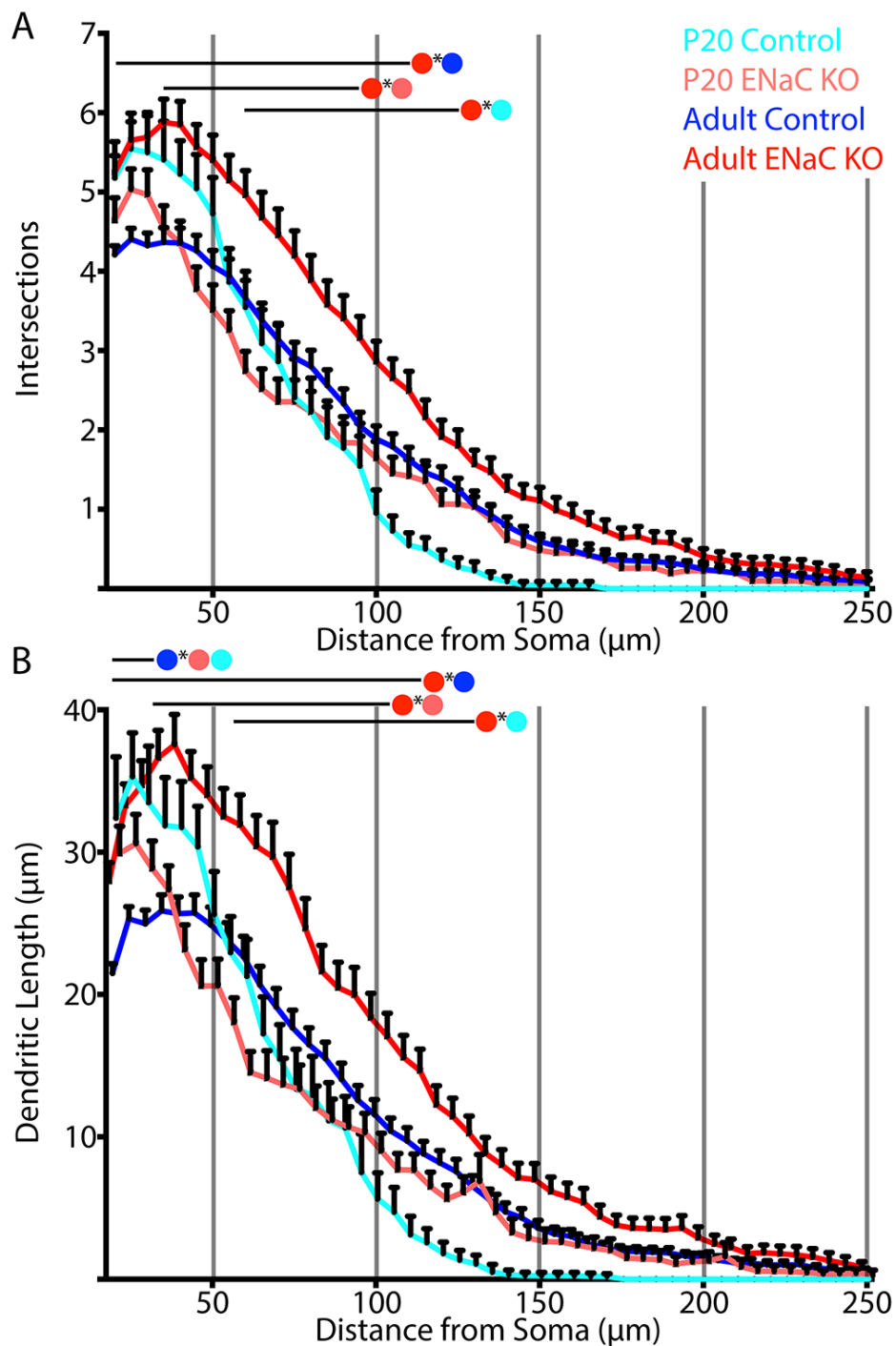


Figure 6. Sholl analysis of NST relay cells. **A**, Number of intersections created by dendrites of NST relay cells from P20 control (light blue), adult control (dark blue), P20 ENaC KO (light red), and adult ENaC KO (dark red) mice as dendrites extend away from the cell soma. **B**, Dendritic length (μm) within each concentric ring created by NST relay cells from P20 control (light blue), adult control (dark blue), P20 ENaC KO (light red), and adult ENaC KO (dark red) mice. Colored circles with lines denote areas of significant difference ($p < 0.05$) between two groups.

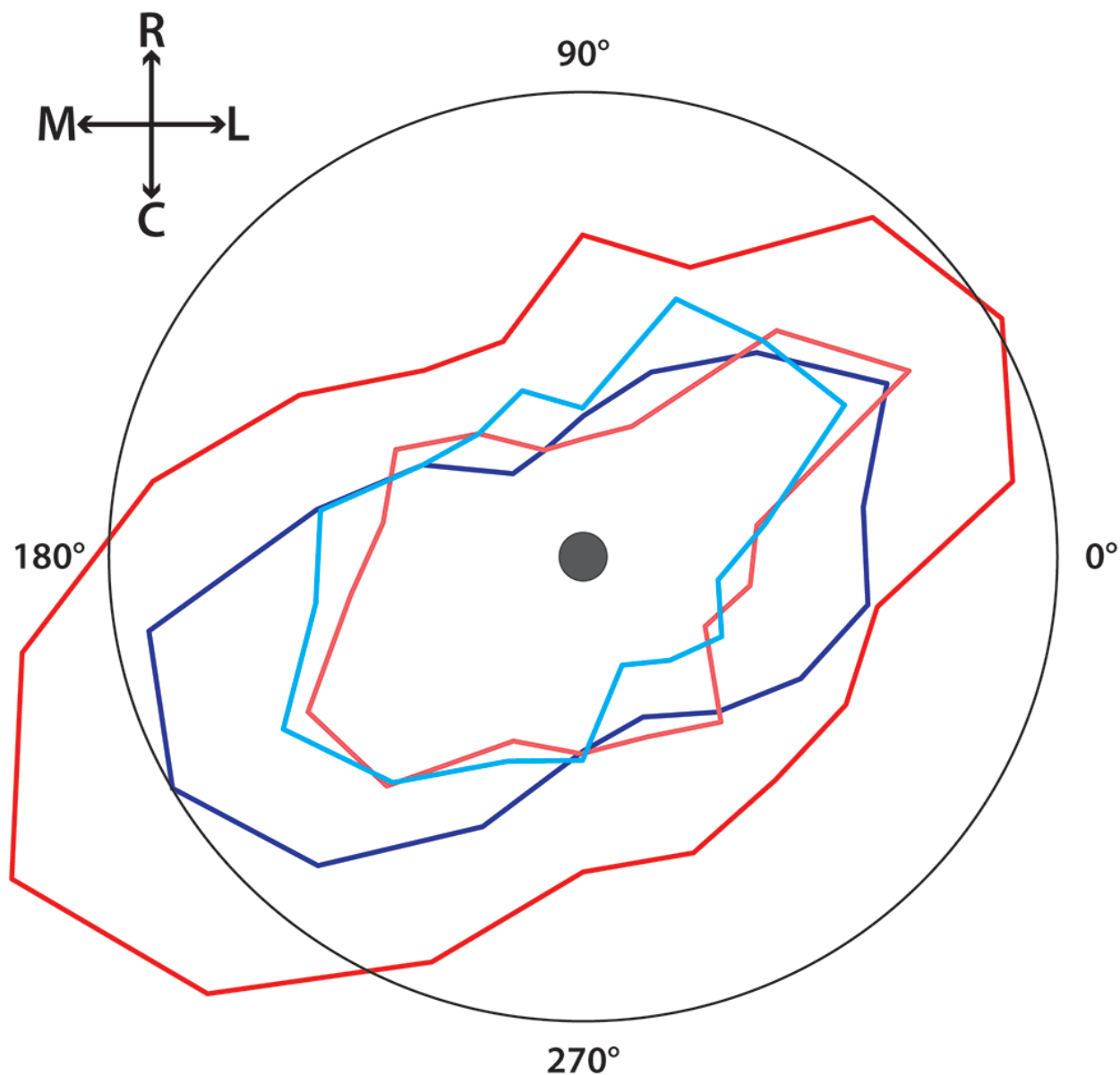


Figure 7. Polar histogram showing the angular distribution of dendritic material in the horizontal plane of cells from P20 control (light blue), adult control (dark blue), P20 ENaC KO (light red), and adult ENaC KO (dark red) mice. Area around the cell soma (grey circle) was divided into 20° bins. The total amount of dendritic material within each 20° bin was measured for each cell and then averaged across each cell group. Mean dendritic lengths for each group within each 20° bin are represented on a relative scale by the distance each point is from the center of the soma. The adult control bin with the largest mean dendritic length (200-220°) was used to normalize all of the other data points. Thus, the black circle represents a normalization ratio of 1. R, rostral; C, caudal; L, lateral; M, medial.

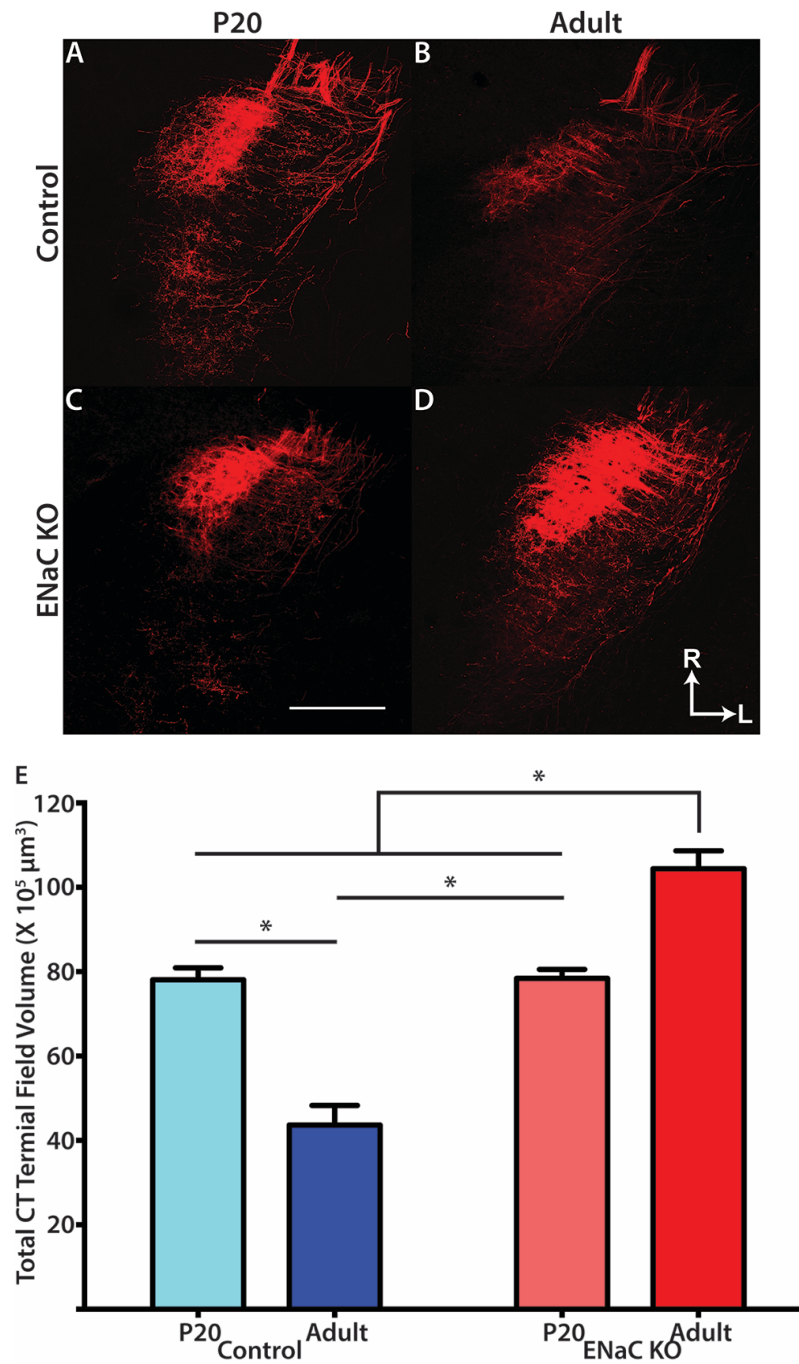


Figure 8. Activity-dependent development of chorda tympani (CT) terminal field. **A-D**, Photomicrographs of the CT terminal field in horizontal sections from a P20 control (**A**), adult control (**B**), P20 ENaC KO (**C**), and adult ENaC KO (**D**) mice. **E**, Quantification of the total CT terminal field volume in P20 control (light blue), adult control (dark blue), P20 ENaC KO (light red), and adult ENaC KO (dark red) mice. * < p 0.05. Scale bar in C, 250μm. R, rostral; L, lateral.

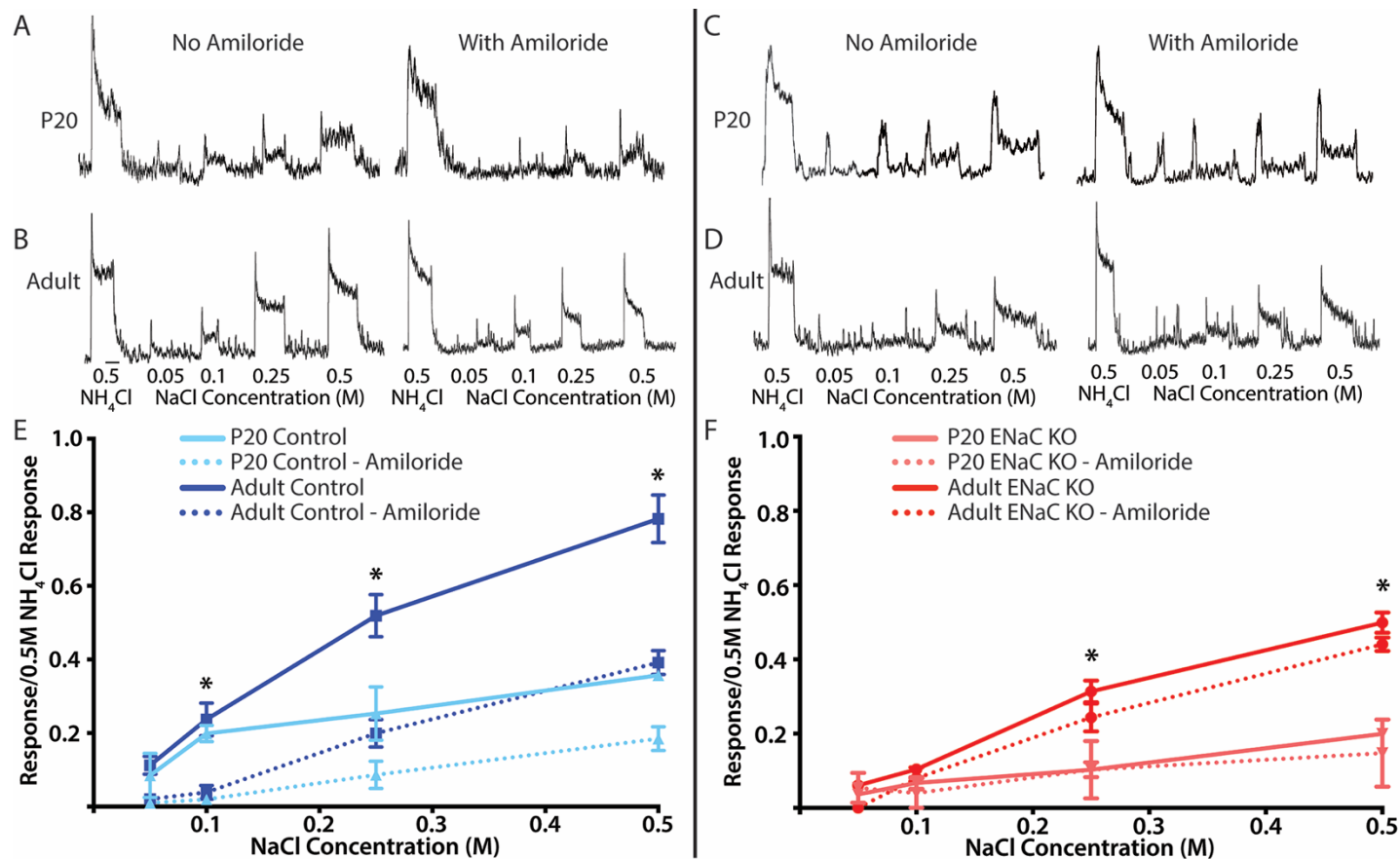


Figure 9. Development of chorda tympani (CT) whole nerve responses in control (left panel) and ENaC KO mice (right panel). **A**, Integrated CT taste responses from a P20 control mouse to 0.5M NH_4Cl and an increasing concentration series of NaCl (0.05, 0.1, 0.25, 0.5M) before and after lingual application of ENaC blocker, amiloride. **B**, Integrated CT taste responses from an adult control mouse to 0.5M NH_4Cl and an increasing concentration series of NaCl (0.05, 0.1, 0.25, 0.5M) before and after lingual application of ENaC blocker, amiloride. **C**, Integrated CT taste responses from a P20 ENaC KO mouse to 0.5M NH_4Cl and an increasing concentration series of NaCl (0.05, 0.1, 0.25, 0.5M) before and after lingual application of ENaC blocker, amiloride. **D**, Integrated CT taste responses from an adult ENaC KO mouse to 0.5M NH_4Cl and an increasing concentration series of NaCl (0.05, 0.1, 0.25, 0.5M) before and after lingual application of ENaC blocker, amiloride. Scale bar in B, 20s. **E**, Mean (\pm SEM) relative taste responses from P20 control mice (light blue) and adult control mice (dark blue) to a concentration series of NaCl before (solid lines) and after (dotted lines) lingual application of amiloride. **F**, Mean (\pm SEM) relative taste responses from P20 ENaC KO mice (light red) and adult ENaC KO mice (dark red) to a concentration series of NaCl before (solid lines) and after (dotted lines) lingual application of amiloride. * < p 0.05

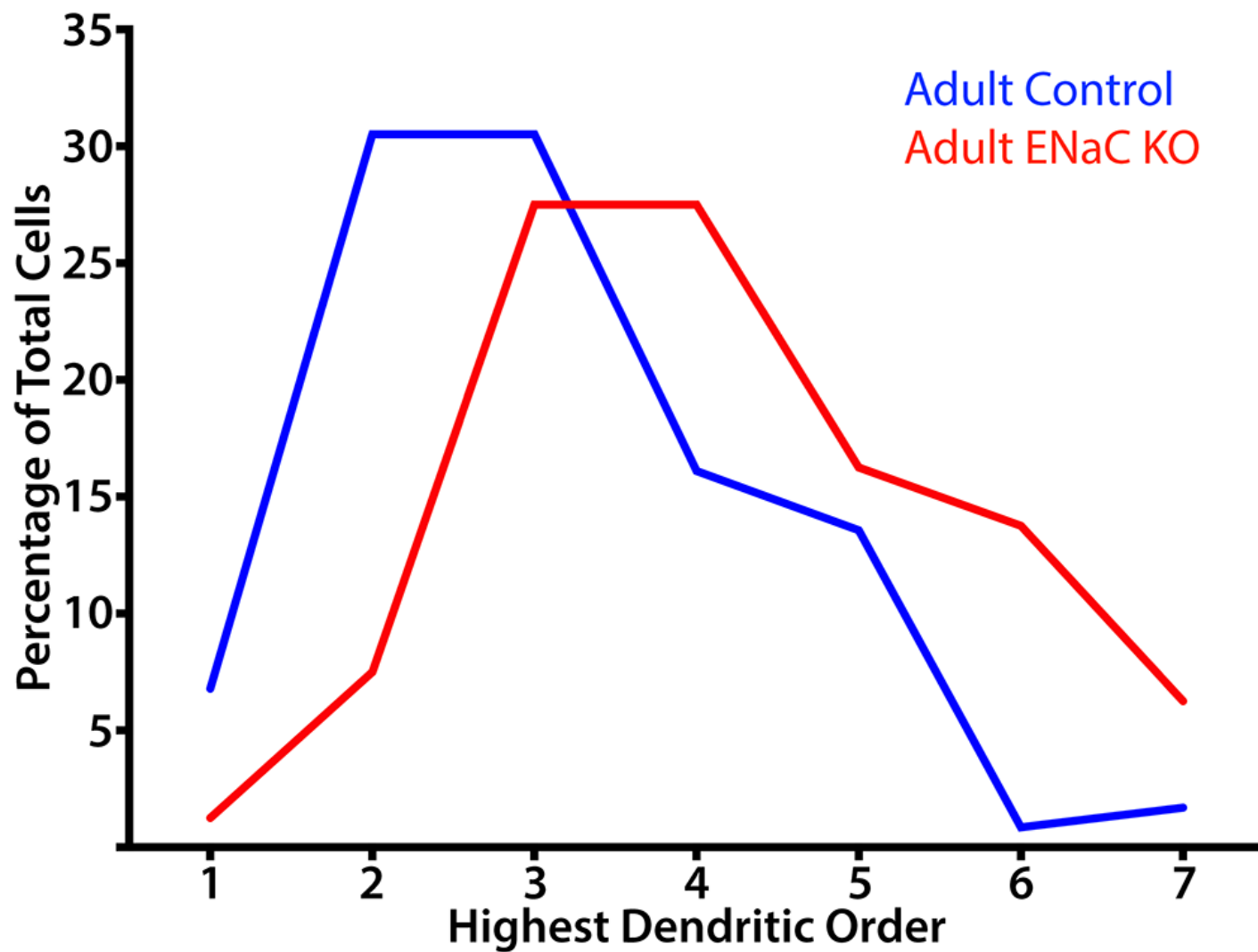


Figure 10. Percentage of total cells by the highest dendritic order expressed within each cell for NST relay cells from adult control (dark blue) and adult ENaC KO (dark red) mice.

Chapter 3: Discussion and Comparison to Other Sensory Systems

The roles of neural activity on the organization of sensory system circuits throughout the central nervous system have become a focus of researchers ever since work by Wiesel and Hubel (1963). In these seminal papers, Wiesel and Hubel (1963) raised kittens in the dark and found deficits in both the anatomy and physiology of cells in the dorsal lateral geniculate nucleus (dLGN) and visual cortex, suggesting that visually-evoked activity plays a role in the development of visual circuits. Since this work, researchers have begun to understand both the multiple roles sensory-evoked neural activity play in the organization of sensory circuits throughout the central nervous system as well as the specific mechanisms that regulate this plasticity. This dissertation, along with previously published data, determines specific roles for ENaC-mediated sodium taste activity on the development, maintenance, and organization of gustatory circuits in the rostral nucleus of the solitary tract (rNST) in the medulla. We report here and previously, that the terminal fields of gustatory afferents require ENaC-mediated sodium taste activity to develop properly (Sun et al., 2017) and to be maintained in a mature state once developed (Skyberg et al., 2017). We also report that the dendritic fields postsynaptic to these gustatory terminal fields require the same neural activity to be maintained at a mature state. Interestingly, our investigation of dendritic architecture of NST relay cells in immature P20 animals suggests that the development of these dendritic fields do not depend on sodium taste activity in the same way that terminal fields do before P20. Excitingly, the effects of removing taste-elicited neural activity in gustatory system are much different to the effects reported to

occur in other developing sensory systems. Here, I will compare and contrast some of the reported effects of ectopically altering neural activity in other sensory systems to what we report here. While the effects of altering neural activity have been categorized in many neural circuits, they are arguably best understood in the visual and auditory systems. Therefore, I will focus this discussion on comparing and contrasting these two model systems to the effects we report in the gustatory system.

Visual System

The roles of neural activity in development and organization of sensory circuits are arguably best characterized in the visual system. This is due, in part, to the relative ease of altering sensory input to the visual system via use of sensory deprivation protocols such as dark rearing, ocular suturing, and genetic knockout mouse models (Wiesel and Hubel, 1963; Feng and Rogowski, 1980; Friedlander et al., 1982; Stretavan et al., 1988; Chapman, 2000; McLaughlin et al., 2003; Mrsic-Flogel, 2005; Demas et al., 2006; Wang et al., 2009). Through these techniques, researchers have illustrated that visual activity plays a role in the organization of both subcortical and cortical visual circuits.

The dorsal lateral geniculate nucleus (dLGN) and the superior colliculus (SC) are the first major synaptic relays in the visual pathway after neural activity leaves the retina, and thus play important roles in organizing and processing of visual information. Retinal ganglion cell axons from both eyes project to the dLGN and SC, where they initially create diffuse, overlapping terminal fields (Katz and Shatz, 1996; Grubb et al., 2003; McLaughlin et al., 2003; Chandrasekaran et al., 2005; Hooks and Chen, 2006;

Guido, 2008). Through a developmental period, categorized by the presence of both spontaneous- and visual-evoked retinal activity, these terminal fields segregate in eye specific layers (Katz and Shatz, 1996; Grubb et al., 2003; McLaughlin et al., 2003; Chandrasekaran et al., 2005; Hooks and Chen, 2006; Guido, 2008). Pharmacological, surgical, or genetic removal of spontaneous retinal activity prevents the segregation of retinal axons in the dLGN and SC into eye specific layers (Katz and Shatz, 1996; Grubb et al., 2003; McLaughlin et al., 2003; Chandrasekaran et al., 2005; Hooks and Chen, 2006; Guido, 2008), illustrating that neural activity, generated in the retina, is necessary for the normal development of retinogeniculate and retinocollicular projections to occur. Therefore, it seems that both retinal activity and ENaC-mediated taste activity play similar roles in driving the development of sensory afferent terminal fields in subcortical circuits dedicated to visual or gustatory processing, respectively. Interestingly, in both the visual and gustatory circuits, removal of neural activity does not just freeze terminal fields in an immature state. Instead, in the absence of activity, both retinogeniculate and chorda tympani axons continue to grow and elaborate (Chapter 2 Fig 8; Sretavan et al., 1988); suggesting these two populations of sensory afferent neurons may have similar default growth patterns and neural activity competes against this innate growth. Finally, in both systems, neural activity has been suggested to be necessary for the continued maintenance of mature terminal field patterns (Chapman, 2000; Demas et al., 2006; Skyberg et al., 2017).

By comparison, the specific roles retinal activity play in the development and maintenance of dendritic fields postsynaptic to retinal ganglion cell axons in the dLGN

and SC are not as well characterized. Nevertheless, the overall developmental trajectory these dendritic arborizations normally take is understood and is similar to what we report to occur in relay cells in the gustatory NST. While there is a slight overall expansion of the dendritic fields of thalamocortical relay cells during the first three postnatal weeks many aspects of dendritic complexity (number of primary dendrites, number of branch points, dendritic order) remain relatively constant throughout postnatal life (Guido, 2008; El-Danaf et al., 2015). This suggests that despite this small postnatal increase in dendritic field size, thalamocortical relay cell dendritic fields mature early in postnatal life, especially when compared to the development of the presynaptic retinal ganglion cell terminal fields. While there has not been a study specifically investigating the hypothesis that retinal activity maintains thalamocortical relay cell dendritic morphology, a few studies examined the effects of monocular deprivation on the overall morphology of thalamocortical relay cells in the dLGN. These studies find that without this visually-evoked activity, soma size and gross dendritic morphology of thalamocortical relay cells develop abnormally (Wiesel and Hubel, 1963; Guillery, 1973; Friedlander et al., 1982). It is important to note that the magnitude of this effect is far less substantial than what we report in gustatory relay cells within the NST, and the direction of this effect was reversed. That is, removal of visually-evoked activity resulted in less elaborate dendritic arborizations.

While the dendritic development of relay cells in the SC and the roles of activity in this development have yet to be characterized, a few studies have investigated the

activity-dependent development of receptive field properties of these SC relay cells (Chandrasekaran et al., 2005; Mrsic-Flogel, 2005; Wang et al., 2009). Using mice genetically designed to lack spontaneous retinal activity, these studies found significant disruptions in the development of receptive field properties of neurons in the SC that respond to visual stimuli. These activity-induced alterations in the receptive field properties of SC relay neurons could be driven by changes in the dendritic and/or synaptic architecture of these cells. However, further research is necessary to definitively delineate a role for retinal activity in development and maintenance of dendritic architecture of relay cells in the SC and dLGN.

Activity-dependent changes in the dendritic architecture of cortical neurons involved in visual processing have also been reported. However, this literature is full of seemingly conflicting reports as to the specific roles neural activity plays in the organization of cortical dendrites. For example, Coleman and Riesen (1968) report that visual deprivation via dark rearing kittens decreases the length and frequency of dendritic branches of V1 stellate cells. Conversely, Lund et al. (1991) found that visual deprivation through either monocular or binocular suturing eyes in young macaques led to dramatic growth of V1 stellate cell dendrites. Thus, the outcome of altering visual activity seems to be dependent upon the animal species, brain region, and type of visual deprivation being used. The latter is a particularly important factor to consider as some visual deprivations remove all retinal activity (tetrodotoxin administration, optic nerve cut), others remove one specific type of retinal activity (binocular suturing, dark rearing,

$\beta 2^{-/-}$ KO mice), and some only alter the overall pattern of incoming visual information (monocular suturing, *nob* mice).

Auditory System

One remarkably elegant illustration of how altering patterns of neural input can affect dendritic organization come from a series of studies on the chick auditory system. In this circuit, auditory information from the cochlea is processed by a series of nuclei in the brainstem before projecting to the thalamus and higher cortical structures. The third-order nucleus, the nucleus laminaris (NL), is a particularly interesting auditory brainstem nucleus as it is the first point in the auditory circuit in which cells receive bilateral auditory input. Axons carrying auditory information from the ipsilateral and contralateral nucleus magnocellularis (NM), the second-order auditory nucleus, preferentially synapse onto the dorsal and ventral dendrites of NL cells, respectively (Sorensen and Rubel, 2011). Usually, the dorsal and ventral dendritic domains of these cells are relatively symmetrical; however, by artificially stimulating either the ipsilateral or contralateral NM, Sorensen and Rubel (2011) were able to induce dendritic asymmetry in NL cells. When they stimulated only the ipsilateral NM, the NL cells responded by retracting their ventral dendrites and elaborating their dorsal dendrites. If they instead stimulated only the contralateral NM, the ventral dendrites became more elaborate while the dorsal dendrites retracted. Importantly, concurrent stimulation of the ipsi- and contra-lateral NM did not produce significant changes in either the dorsal or ventral NL cell dendritic architecture. Therefore, simply increasing the amount of neural activity that NL cells receive is not sufficient to induce dendritic changes;

however, altering the overall pattern of neural activity that NL cells experience, by increasing the activity onto either their dorsal or ventral dendritic domains, is sufficient. Research has also shown that the dendritic architecture of these NL cells, as well as the dendritic architecture of cells in other auditory brainstem nuclei, are dependent upon afferent input for proper development and maintenance to occur (Benes et al., 1977; Feng and Rogowski, 1980; Parks, 1981; Deitch and Rubel, 1984, 1989; Parks et al., 1987; Russell and Moore, 1999). Collectively these experiments suggest that decreasing activity in this system generally results in decreases in dendritic architecture while increasing activity tends to result in dendritic elaboration.

Concluding Remarks

Comparing the specific ways in which neural activity can alter the development and organization of sensory circuits throughout the central nervous system results in a few interesting observations. First, it seems that the effects of removing neural activity in the gustatory system on dendritic architecture are opposite to what has been reported from other sensory systems. That is, removal of neural activity in other sensory systems generally results in loss of dendritic material, especially when investigating subcortical sensory circuits. However, we report here that removal of gustatory activity, specifically sodium taste activity, leads to a substantial increase in the amount of dendritic material and overall dendritic complexity of relay cells in the gustatory NST. While a compelling reason for these differences is not readily apparent, a few potential explanations exist. It could be that removing sodium taste activity is acting to alter the overall pattern of neural activity that NST relay cells experience, similar to the

experiments in the chick auditory system described above. In fact, these relay cells receive input from multiple gustatory transduction pathways, multiple gustatory afferent nerves, and in some cases are multimodal by nature (Hill et al., 1983; Grabauskas and Bradley, 1996; Sato and Beidler, 1997; Cho et al., 2002; Carleton et al., 2010). Thus, it is safe to assume that these relay cells are experiencing some level of neural input even when sodium taste is genetically removed throughout life. Consequently, these changes in NST relay cell dendritic architecture may be more a result of altering the pattern of overall activity these cells experience. Alternatively, the differences in the ways these sensory subcortical structures respond to diminished neural input may be due to differences in the ways these nuclei normally organize incoming neural activity. In vision and audition, afferent inputs onto subcortical circuits are highly spatially organized. For example, visual activity from adjacent retinal ganglion cells will activate adjacent relay cells in the dLGN and/or SC, while visual activity from distal retinal ganglion cells will activate distal dLGN and/or SC relay cells. The auditory environment is similarly topographically mapped onto cells within various auditory brainstem nuclei so that auditory stimuli with similar frequencies are represented by neighboring cells. In this way, important spatial information about the visual and auditory environments are preserved so that our percepts may accurately reflect the environment. Thus, if dendrites of cells in these retinotopic and tonotopic maps become more elaborate when lacking sufficient neural input, they may be decreasing the resolving power (i.e. ability to differentiate two tones or two points of light) of the topographic maps which they are a part of. By comparison, a “chemotopic” map in the

NST has not been discovered, nor does it seem necessary, as the gustatory environment is not spatially organized like the visual and auditory environments. As a consequence, it may actually be beneficial for these cells to become more elaborate when neural input is lacking, as this may increase their ability to detect and summate weak taste activity.

A second observation from this comparison of sensory systems is that the gustatory NST circuit seems to exhibit an unusual level of plasticity, especially for a subcortical sensory nucleus. While it is true that removing sensory-evoked neural activity alters the organization of many subcortical sensory circuits throughout the brain, the magnitude of these effects were far less drastic to what we report here. We show that removing sodium taste activity throughout life results in NST terminal and dendritic fields that are roughly 200-400% larger than in age matched controls. By comparison, removing spontaneous retinal activity only leads to retinogeniculate terminal fields that are ~5-15% larger than in age matched controls (Demas et al., 2006). Additionally, the magnitude of dendritic change reported to occur in the dLGN when neural input is removed is far less than what we report in the gustatory NST (Wiesel and Hubel, 1963; Guillery, 1973; Friedlander et al., 1982). Finally, while it has been reported that neural activity is necessary for the maintenance of dLGN circuits, there is some debate in the field to the extent to which this is true. Some studies claim there is a critical period in which activity must act to induce this circuit plasticity (McLaughlin et al., 2003; Hooks and Chen, 2007), while others suggest that activity can act to alter dLGN organization throughout life (Chapman, 2000; Demas et al., 2006). While the level of adult plasticity this circuit exhibits may still be up for debate, it is clear that the visual

circuit is more plastic early in life than it is in adulthood. By comparison, gustatory circuits in the NST exhibits a far greater dependence on neural input to develop and be maintained properly throughout an animal's life (Chapter 2; Skyberg et al., 2017; Sun et al., 2017). The differences in the level of plasticity these sensory systems exhibit are likely manifestations of differences in anatomy, physiology, and/or function. For example, one unique property of the gustatory system is that taste buds turnover about every 10 days (Beidler and Smallman, 1965; Hamamichi et al., 2006). This results in ever changing receptive fields of the same neurons in which we show a lifelong terminal field plasticity. That is, both the peripheral and central limbs of these gustatory afferents exhibit lifelong plasticity. If the goal of primary afferent neurons is to reliably relay sensory information from the periphery to the central nervous system, and the peripheral organization is constantly changing, then one might expect plasticity in the central nervous system to reflect these lifelong peripheral changes.

While future research will be necessary to fully delineate the mechanisms that underlie the differences in plasticity these sensory systems exhibit, one similarity is glaringly obvious; all sensory systems have to ability to change in the presence of neural input. In fact, this is more generally a characteristic of nervous systems than it is of sensory systems. The ability to change anatomically in response altered physiology is one of the mechanisms by which our brains master coordinated complex movements and skills, learn languages and speech, acquire and change memories, respond to injury, and alter our perceptions of the world. At its worst, this neuroplasticity can lead to maladaptive behaviors like addiction and has been associated with neurological

conditions such as amblyopia, neuropathic pain, and autonomic dysreflexia (O'Brien, 2009; Brown and Weaver, 2016; Tailor et al., 2017). At its best, it grants us the ability to successfully interact with the changing worlds in which we live.

Citations

Beidler LM, Smallman RL (1965) Renewal of cells within taste buds. *J Cell Biol* 27:263–272.

Benes FM, Parks TN, Rubel EW (1977) Rapid dendritic atrophy following deafferentation: An EM morphometric analysis. *Brain Res* 122:1–13.

Brown A, Weaver LC (2016) The dark side of neuroplasticity. *Exp Neurol* 235:133–141.

Cang J, Rentería RC, Kaneko M, Liu X, Copenhagen DR, Stryker MP (2005) Development of precise maps in visual cortex requires patterned spontaneous activity in the retina. *Neuron* 48:797–809.

Carleton A, Accolla R, Simon S (2010) Coding in the mammalian gustatory system. *Trends Neurosci* 33:326–334.

Chandrasekaran AR, Plas D, Gonzalez E, Crair MC (2005) Evidence for an Instructive Role of Retinal Activity in Retinotopic Map Refinement in the Superior Colliculus of the Mouse. *J Neurosci* 25:6929–6938.

Chapman B (2000) Necessity for Afferent Activity to Maintain Eye-Specific Segregation in Ferret Lateral Geniculate Nucleus. *Science* (80-) 287:2479–2482.

Cho YK, Li C-S, Smith D V (2002) Taste responses of neurons in the hamster solitary nucleus are modulated by the central nucleus of the amygdala. *J Neurophysiol* 88:2979–2992.

Deitch JS, Rubel EW (1984) Afferent influences on brain stem auditory nuclei of the chicken: Time course and specificity of dendritic atrophy following deafferentation. *J Comp Neurol* 229:66–79.

- Deitch JS, Rubel EW (1989) Rapid Changes in Ultrastructure During Deafferentation-Induced Dendritic Atrophy. *J Comp Neurol* 281:234–258.
- Demas J, Sagdullaev BT, Green E, Jaubert-Miazza L, McCall MA, Gregg RG, Wong ROL, Guido W (2006) Failure to Maintain Eye-Specific Segregation in nob, a Mutant with Abnormally Patterned Retinal Activity. *Neuron* 50:247–259.
- El-Danaf RN, Krahe TE, Dilger EK, Bickford ME, Fox MA, Guido W (2015) Developmental remodeling of relay cells in the dorsal lateral geniculate nucleus in the absence of retinal input. *Neural Dev* 10:1–17.
- Feng AS, Rogowski BA (1980) Effects of monaural and binaural occlusion on the morphology of neurons in the medial superior olivary nucleus of the rat. *Brain Res* 189:530–534.
- Friedlander MJ, Stanford LR, Sherman SM (1982) Effects of monocular deprivation on the structure-function relationship of individual neurons in the cat's lateral geniculate nucleus. *J Neurosci* 2:321–330.
- Grubb MS, Rossi FM, Changeux JP, Thompson ID (2003) Abnormal functional organization in the dorsal lateral geniculate nucleus of mice lacking the beta 2 subunit of the nicotinic acetylcholine receptor. *Neuron* 40:1161–1172.
- Guido W (2008) Refinement of the retinogeniculate pathway. *J Physiol* 586:4357–4362.
- Guillery RW (1973) Quantitative studies of transneuronal atrophy in the dorsal lateral geniculate nucleus of cats and kittens. *J Comp Neurol* 149:423–437.
- Hamamichi R, Asano-Miyoshi M, Emori Y (2006) Taste bud contains both short-lived and long-lived cell populations. *Neuroscience* 141:2129–2138.

- Hill DL, Bradley RM, Mistretta CM (1983) Development of taste responses in rat nucleus of solitary tract. *J Neurophysiol* 50:879–895.
- Hooks BM, Chen C (2006) Distinct Roles for Spontaneous and Visual Activity in Remodeling of the Retinogeniculate Synapse. *Neuron* 52:281–291.
- Hooks BM, Chen C (2007) Critical periods in the visual system: changing views for a model of experience-dependent plasticity. *Neuron* 56:312–326.
- Katz L., Shatz CJ (1996) *Synaptic Activity and the Construction of Cortical Circuits*. Science (80-) 274:1133–1138.
- McLaughlin T, Torborg CL, Feller MB, O’Leary DDM (2003) Retinotopic map refinement requires spontaneous retinal waves during a brief critical period of development. *Neuron* 40:1147–1160.
- Mrsic-Flogel TD (2005) Altered Map of Visual Space in the Superior Colliculus of Mice Lacking Early Retinal Waves. *J Neurosci* 25:6921–6928.
- O’Brien CP (2009) Neuroplasticity in addictive disorders. *Dialogues Clin Neurosci* 11:350–353.
- Parks TN (1981) Morphology of axosomatic endings in an avian cochlear nucleus: Nucleus magnocellularis of the chicken. *J Comp Neurol* 203:425–440.
- Parks TN, Jackson H, Conlee JW (1987) Axon-target cell interactions in the developing auditory system. In: *Current Topics in Developmental Biology* (Moscona AA, Monroy ABT-CT in DB, eds), pp 309–340. Academic Press.
- Russell A, Moore D (1999) Effects of unilateral cochlear removal on dendrites in the gerbil medial superior olivary nucleus. *Eur J Neurosci* 11:1379–1390.

Sato T, Beidler LM (1997) Broad tuning of rat taste cells for four basic taste stimuli.

Chem Senses 22:287–293.

Skyberg R, Sun C, Hill DL (2017) Maintenance of Mouse Gustatory Terminal Field

Organization is Disrupted Following Selective Removal of Peripheral Sodium Salt

Taste Activity at Adulthood. J Neurosci 37:7619–7630.

Sorensen SA, Rubel EW (2011) Relative input strength rapidly regulates dendritic

structure of chick auditory brainstem neurons. J Comp Neurol 519:2838–2851.

Sretavan DW, Shatz CJ, Stryker MP (1988) Modification of retinal ganglion cell axon

morphology by prenatal infusion of tetrodotoxin. Nature 336:468–471.

Sun C, Hummler E, Hill DL (2017) Selective Deletion of Sodium Salt Taste during

Development Leads to Expanded Terminal Fields of Gustatory Nerves in the Adult

Mouse Nucleus of the Solitary Tract. J Neurosci 37:660–672.

Taylor VK, Schwarzkopf DS, Dahlmann-Noor AH (2017) Neuroplasticity and amblyopia:

Vision at the balance point. Curr Opin Neurol 30:74–83.

Wang L, Rangarajan K V., Lawhn-Heath CA, Sarnaik R, Wang B-S, Liu X, Cang J (2009)

Direction-Specific Disruption of Subcortical Visual Behavior and Receptive Fields in

Mice Lacking the 2 Subunit of Nicotinic Acetylcholine Receptor. J Neurosci

29:12909–12918.

Wiesel TN, Hubel DH (1963) Effects of visual deprivation on morphology and physiology

of cells in the cat's lateral geniculate body. J Neurophysiol 26:978–993.